

xx(1785881)

Algoritmo de Localización de Nodos en Redes de Sensores Inalámbricas Basado en un Modelo Probabilístico y de Escalamiento Multidimensional

**Tesis de Maestría en Ciencias
Ingeniería Eléctrica**

Por:

Ernesto Navarro Alvarez
Ingeniero en Sistemas Computacionales
Instituto Tecnológico de Colima 1996-2001

Becario de Conacyt, expediente no. 203226



**CENTRO DE INVESTIGACIÓN Y
DE ESTUDIOS AVANZADOS DEL
INSTITUTO POLITÉCNICO
NACIONAL**

**COORDINACIÓN GENERAL DE
SERVICIOS BIBLIOGRÁFICOS**

Director de Tesis

Dr. Mario Angel Siller González Pico

CINVESTAV del IPN Unidad Guadalajara, Septiembre de 2008.

**CINVESTAV
IPN
ADQUISICION
DE LIBROS**

CLASIF.: <u>IK16S.48 N38 2008</u>
ADQUIS.: <u>501-527</u>
FECHA: <u>23. III - 2009</u>
PROCED.: <u>Don. 2009</u>
\$ <u> </u>

ID: 158258-1001

Algoritmo de Localización de Nodos en Redes de Sensores Inalámbricas Basado en un Modelo Probabilístico y de Escalamiento Multidimensional

**Tesis de Maestría en Ciencias
Ingeniería Eléctrica**

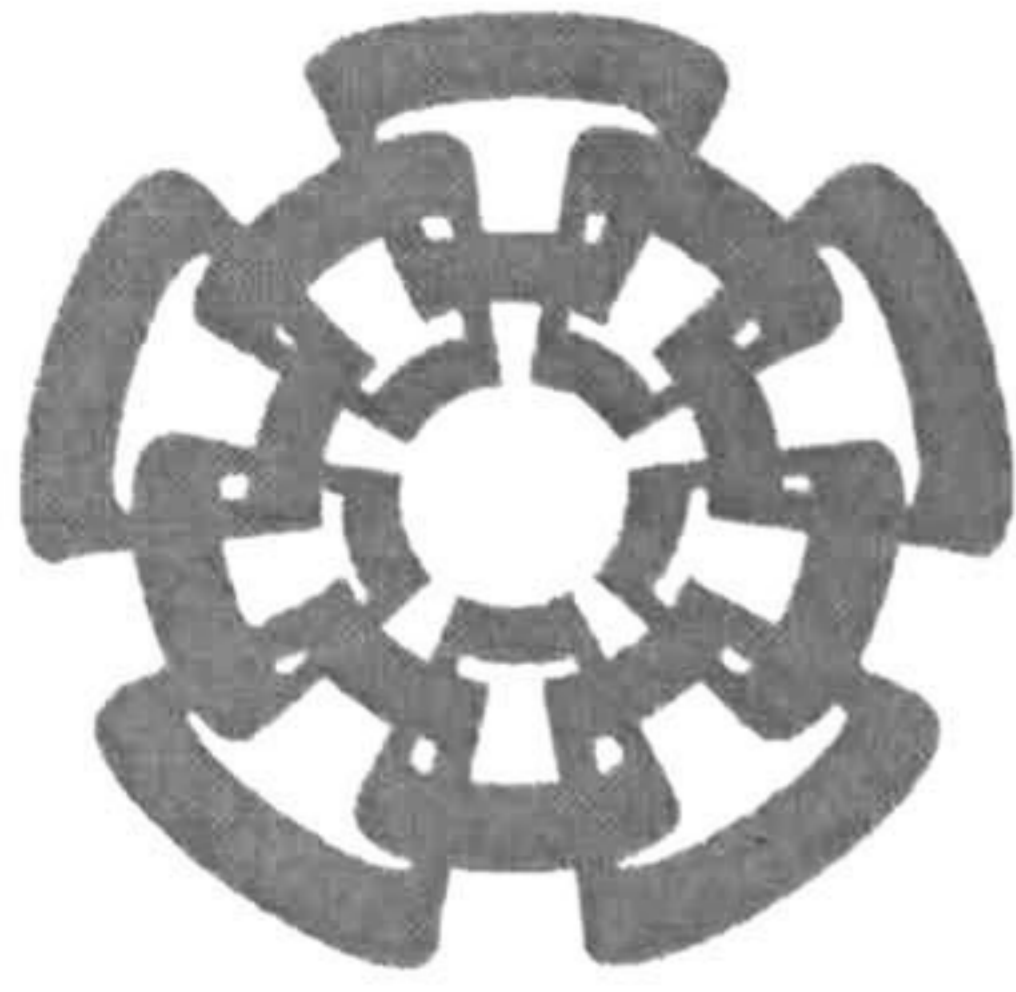
Por:

Ernesto Navarro Alvarez
Ingeniero en Sistemas Computacionales
Instituto Tecnológico de Colima 1996-2001

Becario de Conacyt, expediente no. 203226

Director de Tesis
Dr. Mario Angel Siller González Pico

CINVESTAV del IPN Unidad Guadalajara, Septiembre de 2008.



Centro de Investigación y de Estudios Avanzados
del I.P.N.

Unidad Guadalajara

**An algorithm for node localization in
WSN based on a probabilistic model and
Multidimensional Scaling**

A thesis presented by:
Ernesto Navarro Álvarez

to obtain the degree of:
Master in Science

in the subject of:
Electrical Engineering

Thesis Advisor:
Dr. Mario Ángel Siller González Pico

Guadalajara, Jalisco, September 2008.

An algorithm for node localization in WSN based on a probabilistic model and Multidimensional Scaling

**Master of Science Thesis
In Electrical Engineering**

By:

Ernesto Navarro Álvarez

Engineer in Computer Systems

Instituto Tecnológico de Colima 1996-2001

Scholarship granted by CONACYT, No. 290501

Thesis Advisor:

Dr. Mario Ángel Siller González Pico

CINVESTAV del IPN Unidad Guadalajara, September, 2008.

RESUMEN

Se propone un algoritmo para atacar el Problema de la Localización de un objeto dentro de una red inalámbrica sensorial (WSN) la cual está formada por dispositivos baratos y de exactitud limitada. El algoritmo crea un sistema de coordenadas relativo al aplicar una técnica de Escalamiento Multidimensional (MDS) para encontrar una posición estimada en un plano cartesiano. Dicho plano puede ser a su vez alineado con un sistema global de coordenadas geográficas si se dispone de equipo adicional como un GPS.

El algoritmo que se propone se centra en el uso de la señal de radio frecuencia como única fuente de información. La ventaja de esto radica en que la capacidad de comunicación RF esta presente en cualquier dispositivo inalámbrico. Debido a diversos fenomenos físico (como desvanecimiento, reflexion, lonquitud de camino recorrido, etc.) una señal de radio frecuencia sufre una atenuación en su potencia conforme aumenta la distancia entre emisor y receptor. Este hecho es aprovechado por el algoritmo para obtener una distancia estimada entre receptor y emisor usando la perdida de potencia. En esta estimación se usa un indicador de la fuerza de la señal recibida (RSSI); en nuestro caso de estudio, usamos como indicador el LQI proporcionado por la pila del protocolo ZigBee (estándar de la IEEE 802.15.4).

Sin embargo, la señal tiende a propagarse de manera no uniforme en distintos ambientes, además que contiene ruido que induce errores en la estimación de distancia. Por lo anterior, se han considerado algunos fenómenos físicos que afecta la propagación de la señal tales como: reflexión, patron de radiacion, etc. En particular, se ha encontrado un fenómeno de reflexión conocido como Espejo de Lloyd (el cual causa interferencias destructivas y constructivas para una onda) que origina una variabilidad en la fuerza de la señal recibida.

Abstract

An algorithm for node localization in wireless sensor network (WSN) is proposed. This algorithm produces a relative coordinate system by applying a Multidimensional Scaling Technique (MDS) to find estimated node positions in a Cartesian plane. This plane can be later aligned with global geographic coordinates by using some specialized hardware (e.g. GPS device).

The algorithm uses only connectivity information by taking advantage of the inherent Radio Frequency (RF) communication capability present in each node of the WSN. The RF signal is attenuated as the distance between the transmitter and receiver increases. The algorithm estimates the distance by using the RF signal power. The estimation is carried out from the Received Signal Strength Indication (RSSI).

In the study case the Link Quality Indicator (LQI) is employed and provided by the Zigbee protocol (IEEE 802.15.4). The algorithm is intended for WSNs composed of inexpensive and limited accuracy components.

Acknowledgments

Thanks to my parents Oscar and Rosa.

Thanks to my Thesis advisor Dr. Mario Siller for his guidance.

Thank to Salvador Jauregui for his technical help on GNUplot.

Thanks to CONACYT for the economic support.

Preface

The recent advances in sensors, embedded systems, wireless communications, and miniaturization have made possible a new kind of application in ubiquitous / pervasive computing: *the Wireless Sensor Networks*.

Wireless Sensor Networks can be seen as a collection of small computing devices with limited storage and processing capabilities equipped with low power and cost microcontrollers. These devices can communicate between each other wirelessly and contain the necessary sensors and/or actuators for measuring a physical phenomena and carrying out actions on it.

These small devices can be deployed in a random manner in different physical environments (indoor and outdoor). Their use range over a wide spectrum of applications such as: wildlife and environmental monitoring, target tracking, military surveillance, health patient monitoring etc. For a complete study of all possible applications of WSN see [1]

But, for making the application previously mentioned possible, it is necessary to know where the phenomena are taking place (a physical location is required). The localisation estimation is required for the applications that need to know the geographical origin of events.

A simple but not the cheapest way to solve the localisation problem is adding a GPS device to every sensor. For most of the WSN price and energy consumption would be a drawback for this solution, because of the sensor limited energy source (AA batteries). Also GPS devices have some problems in indoor environments (one possible scenario for WSN) to work well.

This thesis focuses on the use of connectivity information by taking advantage of the inherent Radio Frecuency communication capability present in each node of the WSN to avoid the use of GPS equipment in each sensor.

Contents

1	Introduction	1
1.1	Problem Description	1
1.2	Thesis objective.	2
1.3	Thesis structure	2
2	State of the Art	3
2.1	Introduction	3
2.2	Terminology	3
2.3	Localisation algorithms	4
2.3.1	No-mobility options .	4
2.3.2	Mobility options	6
2.4	Conclusion	10
3	Signal Strength Analysis	11
3.1	Introduction	11
3.1.1	The Zigbee Protocol	11
3.1.2	MC1321x family	11
3.1.3	The Link Quality Indicator (LQI)	12
3.2	The experiment	14
3.2.1	The Design	14
3.2.2	The Data Collection & Analysis	14
3.3	The Lloyd Effect	18

3.4	The antenna radiation pattern	20
3.5	Conclusion	26
4	Development of the proposed algorithm	27
4.1	Introduction	27
4.1.1	Zigbee Protocol Stack	27
4.1.2	Zigbee topologies	28
4.2	Experimental Network Implementation	29
4.2.1	Nodes deployment	29
4.2.2	Building the network topology	29
4.2.3	RSSI Reports	31
4.2.4	The PAN coordinator estimates distances between sensors.	33
4.3	The Localisation Algorithm	34
4.3.1	General description	34
4.3.2	Graph Matrix ($A(Conectivities)$)	35
4.3.3	Distance Matrix ($D = M_{n \times n}(Distances)$)	35
4.3.4	Cross Product Matrix ($B = M_{n \times n}(CrossProduct)$)	35
4.3.5	Singular value decomposition (SVD)	36
4.4	Conclusion	37
5	Experimental Results	39
5.1	Introduction	39
5.2	The localisation algorithm under the use of beacons	39
5.2.1	Simulation	40
5.2.2	Field Experimental Work .	41
5.3	The algorithm without beacons	46
5.3.1	Simulation	46
5.4	Analysis	47
5.5	Conclusions	50

<i>CONTENTS</i>	V
6 Conclusions and Future Work	51
6.1 Conclusions	51
6.2 Future Work .	52
A MC1321x family	53
B Singular Value Decomposition	55
C Mean & StDev for 1-60 mts distance	57
Bibliography	59

List of Tables

3.1	This table summarize common cases of dBm values.[2]	13
3.2	This table summarize the dBi values for 360 degrees	25
5.1	Physical position of the unknown nodes	46
5.2	Estimated position for the unknown nodes	46
5.3	Table of errors of the field experimental work.	46
5.4	Different positions for the beaconless case .	47
5.5	This table summarize errors of distance for the simulation	48
5.6	This table summarize errors on X-axis for the simulation	48
5.7	This table summarize errors on Y-axis for the simulation	49
C.1	This table summarize the mean and StDev for 1 to 40 meters.	57
C.2	This table summarize the mean and StDev for 41 to 60 meters. .	58

List of Figures

2.1	Figure 2.1: a) Angle features representing corners. b) points features representing columns.	9
3.1	The transmitter and receiver sensors in the middle of the Cinvestav soccer field.	15
3.2	RSSI as a function of transmitter-receiver separation derived from the empirical data collected.	15
3.3	Mean, Standard Deviation and median for 1 and 2 meters of RSSI values.	16
3.4	Free space propagation model plotting RSSI values versus distance (Friis Model)	17
3.5	Lloyd's Mirror.	18
3.6	Lloyd Effect vs distance	21
3.7	Theoretical Proposed model vs Experimental Data collected.	22
3.8	(a)Printed F-antenna Radiation Pattern (b)Top view orientation of the MC1321x circuit board. Images taken from [3]	23
3.9	Transmitter placed 1 and 2 meters away from receiver. Receiver rotated 360 degrees.	24
3.10	Transmitter placed 3 and 4 meters away from receiver. Receiver rotated 360 degrees.	26
4.1	Zigbee Protocol Stack by Freescale.	28
4.2	Peer-to-peer topology.	29
4.3	The state diagram for PAN Coordinators	30
4.4	The state diagram for neighbor devices (sensors)	32
4.5	A cluster tree with 3 PAN id. Image taken from [4]	33

5.1	8 beacon sensors layout	40
5.2	Different estimations for one random position	41
5.3	Histograms for the errors	42
5.4	Position 1 result.	42
5.5	Position 2 result.	43
5.6	Position 3 result.	43
5.7	Position 4 result.	44
5.8	Position 5 result.	44
5.9	Position 6 result.	45
5.10	Position 7 result.	45
5.11	Position 8 result.	47
5.12	Different estimations for 4 nodes .	48
5.13	Uncertainty regions bounded by the red boxes	49

Chapter 1

Introduction

1.1 Problem Description

Different definitions for the localisation problem can be found in the related literature. In [5] the localization problem is defined as determining an assignment of coordinates for nodes in a wireless ad-hoc or sensor network that is consistent with measured pair wise node distances. In [6] is defined as determining where a given node is physically located in a network. The localisation problem lies in estimating the position, spatial or geographical coordinates of a node within the Wireless Sensor Network, and can be formally stated as follows:

Given a Graph $G = (V, E, \psi)$ with $|V| = n, |E| = m$ (nodes, labeled 1 through n), and the distance measurements between each pair of nodes $w(\psi(i, j))$, $i, j \in \{1, 2, \dots, n\}$, produce an assignment of vertices V to points in \mathbb{R}^2 (coordinates) x_i for each node i , such that the assigned distance between nodes i, j , $|x_i - x_j|$ equals the measured Euclidian distance $\delta(i, j)$.

The distance measurement mentioned above are obtained via Radio Frequency (RF) Communication between nodes. Because diverse physical phenomenon (like fading, scattering, multipath, etc.) RF signals are attenuated as the distance between the transmitter and the receiver increases. The signals' energy diminishes quadratically with the distance. Knowing the output power of the transmitter and the input power of the receiver, a distance estimated can be calculated. However, the radio signal propagation tends to be non-uniform in different environments. Also, the signal contains noise that may induce errors of several meters in the estimation.

In chapter 4 these errors are limited by using an appropriate propagation model.

1.2 Thesis objective.

The main goal of this thesis is to formulate and develop a general algorithm for node localization in Wireless Sensor Networks able to work under the following conditions:

- It should employ probabilistic techniques to deal uncertainty.
- It should work over a wireless communication protocol based on radio frequency.
- It should use only radio frequency signals to do localization.
- It should not require specialized hardware.
- It should be able to work without the help of anchors nodes (nodes with GPS or nodes whose positions are known and fixed).
- It should take on account the movement of the nodes (mobility).
- It should be able to work without infrastructure (ad-hoc network).
- The output of the algorithm should be map position of the nodes relative to themselves.
- It should be able to work in large scale networks (hundreds or thousands of sensors).

1.3 Thesis structure

The thesis is structure as follow: chapter 2 reviews the state of the art of localization systems; chapter 3 documents the signal strength experiment setup and the experimental data collected; chapter 4 presents the proposed algorithm; chapter 5 presents an experimental result of the proposed solution, and finally chapter 6 presents the conclusions, remark and future work.

Chapter 2

State of the Art

2.1 Introduction

A review of state of the art in localisation algorithms is made. This includes major localisation techniques. A comparison of the different algorithms and some conclusions are presented. Also some basic definitions to the problem are presented.

2.2 Terminology

In a Sensor Network, a node can be one of the two following kinds: a *Beacon* or *Unknown*. The beacon node has a known position (being either placed at known positions or by using a GPS). The unknown node does not know its position, so it has to estimate it with the help of the beacons.

A *range-based algorithm (proximity-based)* is an algorithm that infers the distance (estimation) between nodes based on constraints from the proximity to beacon nodes. These approaches do not require specialized hardware. A range-free algorithm relies on precise range measurements to estimate the position of the unknown nodes.

The distance estimation between pair of nodes is carried out from the Received Signal Strength Indicator (RSSI). *RSSI* is a measurement of the power of the received radio signal by the receiver's circuit and is expressed in dBm units.

2.3 Localisation algorithms

Node mobility is referred to as the node capacity to change its physical location. The localisation problem can be studied in two different contexts in terms of node mobility. The node mobility and the lack of it derive different challenges for the node localisation estimation.

2.3.1 No-mobility options

The algorithms which consider no mobility in the localisation problem are referred to as *static schemes*. The main solutions on this classification are RSSI Based, radio hop count, geometric convex constraints, overlapping Coverage Areas, probabilistic approach and MDS. Other solutions are derived from or the combination of these techniques.

RSSI Based

There are different radio propagation models which are based on the average of the received signal strength from a given transmission distance. Location systems such as Radar System [7] and SpotON [8] use the RSSI signal in indoor environments. SpotON is based on a RFID technology. It uses a long range ID badge from a company named RF Ideas INC to implement the localisation solution. The signal strength measurements and node distance are provided by multiple base stations. These values are then triangulated by a central server to estimate the node location by using the following function.

$$SS = 0.0236*d^2 - 0.629 * d + 4.781 \quad (2.1)$$

This function is derived from empirical data analysis mapping basestation distance (d) to the signal strength estimate (SS). Note that SS is in abstract unit.

One of the main advantages of this approach is that the RSSI is available in any transceiver. However, the main limitation derives from the nonlinearity of the indoors RF signal strength in relation to the distance. Another constraint is the non-Gaussian noise, resulting from multipath and environmental effects, such as building geometry, network traffic, presence of people, and atmospheric conditions [9]. Propagation models (Rayleigh, Hashemi, Rician, etc.) that take into account diffraction, scattering and reflection have been investigated over the past years [10].

Radio Hop Count

This approach is based on the principle that is quite probable that when two nodes communicate using a radio signal the distance between each other is less than the maximum range of their radios, no matter what their signal strength reading is [11]. This is the basics for hop count localisation. This scheme consists in building an unweighted graph representing the connectivity among the different nodes. Once the connection distances are estimated using the previous principle these are assigned as weights to the graph. The assumption on this is that the area coverage capacity is the same for each radio. In [12] the Ad Hoc Positioning System (APS) solution is proposed. It uses hop counts to estimate distance vectors among the node in relation to GPS-landmarks.

Geometric Convex Constraints

Another approach on using radio signal is based on forming geometric constraints around the network nodes [13]. These are referred to as convex regions (bounding). These regions or geometrical shapes characterise the radio signal transmitted by each node. Four geometrical shapes are interpreted from the constraints: radial, angular, quadrant and trapezoid. For the radial constraint the connection between nodes is represented and estimated using a linear matrix inequality (LMI).

Overlapping Coverage Areas

This approach uses a number of fixed beacon nodes for established coverage areas. These nodes are reference points for their neighbour nodes and their positions are known. The use of use of them is limited to whether it is possible to place them in these known locations. The beacons transmit packet with their position every certain period T . These transmissions are synchronized and no overlapping is allowed. The neighbours use this information to calculate a connectivity metric. Then they locate themselves using the intersection areas of the coverage regions of the beacons. The intersection area is referred to as centroid. The signal propagation assumed in this approach is an idealized radio model consisting of: i) perfect spherical radio propagation and ii) identical transmission power for all radios. This solution was proposed by Bulusu et al in [14].

Probabilistic Approach

The estimation on this approach is based on an a priori probabilistic density function (PDF) [15]. This function is derived from RSSI vs. distance measurements. An RSSI measurement is considered as a random variable because of the effects of environmental conditions, errors,

noise, fading, disturbs, etc. For the measurements performed in [15] the PDF of RSSI vs. distance follows a Gaussian distribution. The algorithm is as follows. Each unknown node estimates its initial position. This estimate is updated as new packets are received from fixed beacons or from neighbour nodes. If the new estimate improves the previous one then it is broadcasted to its neighbours after a certain period of time T .

Multidimensional Scaling

MDS is a data analysis technique from mathematical psychology, invented by Torgeson in 1952 who gave the preliminary ideas [16]. Since then many investigators have developed different varieties of MDS like nonmetric MDS, weighted MDS, iterative MDS, qualitative MDS, etc. [17] uses an iterative variant multidimensional scaling (MDS) to compensate for missing inter-node distance. This iterative variant is close related to standard iterative least squares algorithm. A main disadvantage of MDS technique is that it takes $O(n^3)$ time for a network of n nodes [17]. A deeper study is necessary to investigate how to lower this complexity.

2.3.2 Mobility options

The algorithms presented in the previous section do not consider mobile nodes but they could be applied over periods of time. However, the processing costs make this alternative not suitable for sensor networks. Besides the node position change knowledge is not used to improve their localisation. This is not the case for the algorithms discussed in this section. The estimation under this new scenario is done using probabilistic tools. The main reason for this is the uncertainty caused by node mobility characterised by the speed and move directions. A powerful tool used to manage uncertainty in both RSSI measurements and location of the nodes due to mobility is a Bayesian-filter.

The Bayesian inference theory allows modelling the uncertainty of logical inference processes by incorporating prior knowledge from observational evidence. In the localisation problem we must adopt the state space approach to model the mobility of the nodes in a WSN as dynamic system. This dynamic system evolves according to a discrete time. The RSSI measurements are available at discrete time. In this approach two models are required: the dynamic model (or movement model) and the measurement model. -both are formulated in a probabilistic form. In WSN movement models for Mobile Ad-Hoc Networks (MANET) are employed. A survey of these models is presented in [18].

At this stage Bayesian Filtering is used to estimate the dynamics of the system from observations (measurements). The state represents the sensor location. An a priori probability density function (PDF) is then built of the current state x_t based on the previous state x_{t-1} (markov assumption) and all collected measurements up to current time t ($Z_t = z_1, \dots, z_t$).

PDF has all information needed to obtain an estimated of the state. But a new estimate is required every time a new measurement is available. Bayes Filter is executed recursively. The has two important steps: **prediction** and **update**.

In the prediction step the movement model is used, $p(x_t|x_{t-1}, v_{t-1})$ to predict a PDF $p(x_t|Z_{t-1})$. Where x_t is the current state of the system, x_{t-1} is the previous state and v_{k-1} is a performed action. It can be seen that it is specified as a conditional density. Now suppose we already have the PDF $p(x_{t-1}|Z_{t-1})$ which is the previous sate distribution. Then we can integrate the following formula to predict the density of the system state at time t [19].

$$p(x_t|Z_{t-1}) = \int p(x_t|x_{t-1}, v_{k-1})p(x_{t-1}|Z_{t-1})dx_{t-1} \quad (1)$$

In the update step, both the measurement model and new information from the sensor to compute the posteriori PDF $p(x_t|Z_t)$ are used. Now we use the Bayes Rule to compute this updated PDF.

$$p(x_t|Z_t) = \frac{p(z_t|x_t)p(x_t|Z_{t-1})}{p(z_t|Z_{k-1})} \quad (2)$$

These steps are repeated recursively until an optimal estimation is obtained. A useful criterion is the mean-square error, see [19].

A review of some of the localisation algorithms based on Bayesian filters is presented next.

Kalman Filter Approach

The Kalman filter is a variant of Bayes Filter and often used in localisation. This filter assumes that the movement model, measurement model, initial state, and posteriori PDF are Gaussian. Because this assumption KF can't deal with ambiguous situations (multi-modal distribution); however, the sensor location can be easily characterized by its mean a covariance, see equation (3), μ is the mean (1st moment). Σ is the $d \times d$ covariance matrix (2d moment) and d is the state dimension (coordinate position) [20].

$$N(x; \mu, \Sigma) = |2\pi\Sigma|^{-1/2} \exp\{-1/2(x - \mu)^T \Sigma^{-1} (x - \mu)\} \quad (3)$$

The Kalman filters are well-suitable when the dynamic model (or movement model) and the measurement model are both linear. If these models are no linear and multiples beliefs are considered then the Extended Kalman Filter can be employed.

Particle Filter Approach

In this approach, the PDF is represented by a set of samples (also called *particles*). This set is a discrete representation of the continuous distribution. The goal is to randomly and recursively compute the set of samples $S_k = \{S_k^i; i = 1, 2, \dots, N\}$ from the density function $p(x_k|Z_k)$. The Bayesian prediction and update on this approach is performed as described next:

This sample approximates a random sample from the predictive density $p(x_k|z_{k-1})$. This new set doesn't include the sensor measurement at time k . In the update phase a new measurement z_k is included. Each of the samples in S_k is weighted by $m_k^i = p(z_k|S_k^i)$. S_k is then obtained by re-sampling from this weighted set such as that from $j = 1$ to $j = N$ one S_k sample s_k^j is drawn from $\{s_k^i, m_k^i\}$ [21]. This approach takes advantage of mobility to improve the localization precision and accuracy. A key advantage is that it can represent arbitrary probability densities.

However, a drawback is that the number of particles can extend to infinity. Therefore a finite and restricted number of them must be considered. This can be achieved by designing an efficient sampling a re-sampling method. Some solution based in particle filter are: SIR filter, Monte Carlo filter, Condensation, etc.

Grid-Based Approach

This technique estimates the sensor position and orientation in a metric model of the environment. This approach was first used in the field of localisation for mobile robots [22]. The basic idea is to divide the environment into a small grid cell, typically between 10 cm and 1 m in size [20]. This grid is the basis for the approximation of the position probability density $p(x_k|Z^k)$. For each grid cell the probability that it is the current position of the sensor is estimated. A main advantage of this approach is that it can deal with multimodal and non-Gaussian densities at a fine resolution (as opposed to the above discrete methods). However, a drawback is the high memory and processing requirements to store the probability position grids and updated for every new observation. This approach is also known as Occupancy Grids.

Multihypothesis Approach

This approach [23] differs from the others in the sense that it is feature-driven rather than location-driven. Features indicate where to place a location hypothesis. Within the algorithm there can be as many hypotheses as necessary. A feature is defined as a geometric representation of a given object in a plane located in a robot or sensor trajectory. For example, a feature can be an angle representing a corner, a point modelling columns or a line

indicating a wall, see Figure 2.1.

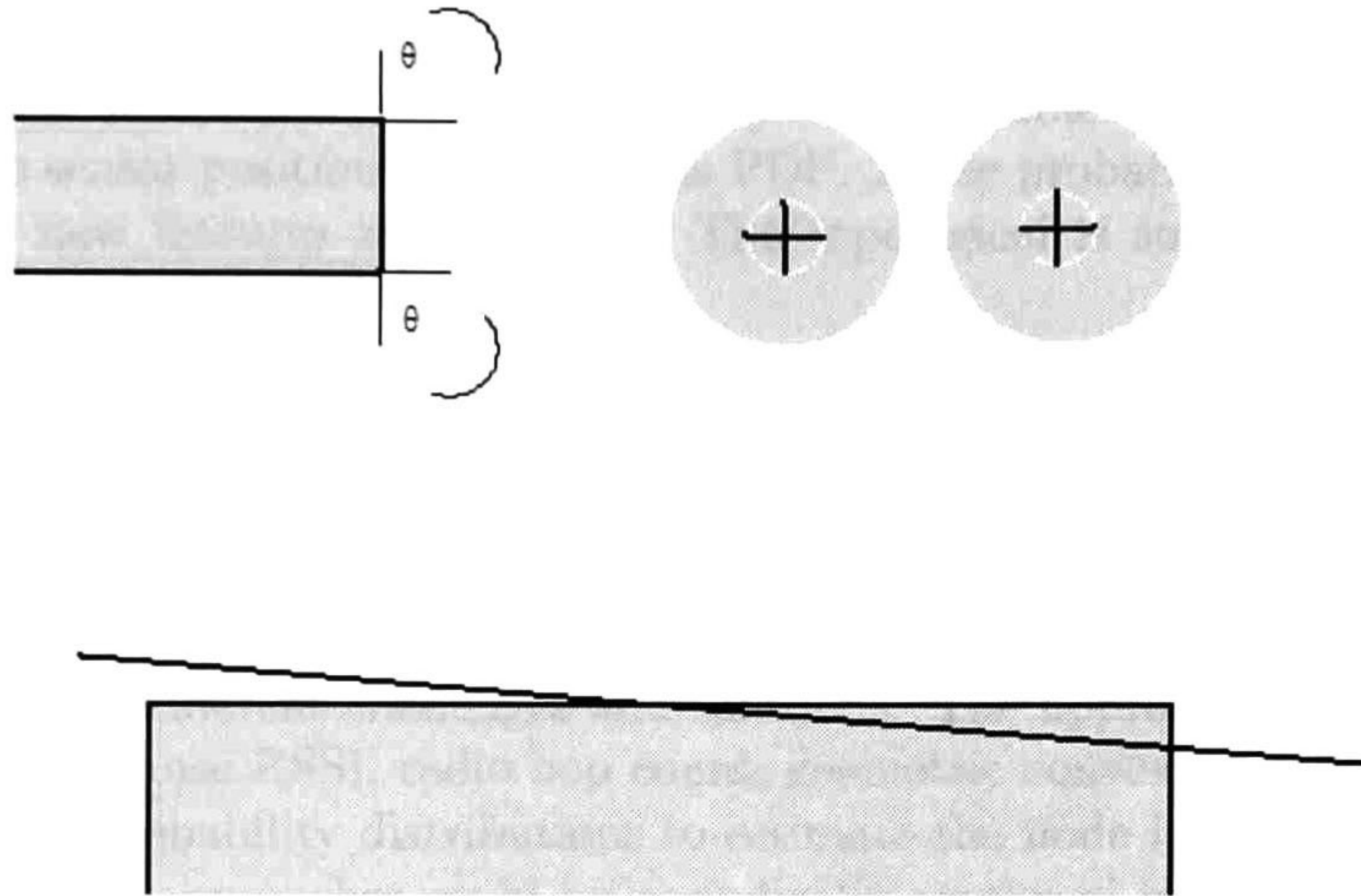


Figure 2.1: Figure 2.1: a) Angle features representing corners. b) points features representing columns.

This approach is based in two maps: a local map of the observed features and a global map for the model features. From these two maps an association (paring) is established between local and global features, $p_{ij} = l_i, g_j$. The observed features are represented by $\{l_1, l_2, ..l_l\}$ whilst model features by $\{g_1, g_2, ..g_m\}$. Based on this an interpretation tree is generated representing all possible associations. A geometric constraint is a physical property between two pairings. There two types of constraints: unary constraints and binary constraints. The former are fundamental properties of a feature such as colour, texture, etc. The latter apply to two features and it can be for example a measure between features like distance or angle. The constraints are used to reduce the search space in the interpretation tree.

Therefore the solution derives from formulating a matching using these geometrics to find the correct set of associations within the space of all possible associations. Since this finding is difficult multiple sets of hypothesis are thus formulated. The number of hypothesis depends on the number of similar features. The reduction of them is derived from geometric constraints and the depth-first back tracking heuristic.

Topological Markov Approach

The main idea is to represent the environment with a graph where nodes represent landmarks or predefined positions or location of the sensor and edges represent the connectivity of corridors or hallways. This graph contains the topology information derived from the node

connectivity, approximate distance (obtained from RSSI measurements and features about the environment like corridor, doorway, etc.). This information can be integrated in Partially Observable Markov Decision Process (POMDP) [24] or Hidden Markov Model (HMM) models [25]. These models maintain a probability density of all possible nodes location in the graph and estimate the sensor positions based on this PDF. These probabilities are updated as the sensor moves or new features are observed. The topological is suitable in applications in which uncertainty is high [15].

2.4 Conclusion

The localisation problem can be studied in two different contexts in terms of node mobility. Each context derives different challenges and solutions. The approaches in which node mobility is not considered use RSSI, radio hop count, geometric convex constraints, overlapping coverage areas and probability distributions to estimate the node location. When node mobility arises the static approaches could be periodically employed but are not suitable under this context because of the required processing power. An alternative to solve the mobility uncertainty is the use of statistical and probability tools such as Bayesian inference theory. For this two models are required to consider the movement and the measurement model. The dynamic approaches result from the application of any variant of Bayesian filters using a given probability distribution. The efficiency and applicability of any static or dynamic algorithm is determined by its characteristics (probability distribution, granularity, range, environment, etc.). They define the estimation precision, network architecture and required power consumption. The localisation solutions presented consider assumptions which are made to simplify the problem such as the radio frequency propagation model and probability distribution. However, these assumptions may not be necessarily accurate to the physical scenario. Therefore different precision estimation may be achieved and it still is an opened research area.

Chapter 3

Signal Strength Analysis

3.1 Introduction

This chapter explains the setup of the experiment designed to model relation between RSSI and distance. It also introduces theoretical concepts related to the experiments.

3.1.1 The Zigbee Protocol

ZigBee is a low data rate, low power consumption, low cost, wireless networking protocol targeted towards automation and remote control applications. This protocol is based in the IEEE 802.15.4 standard. Zigbee is also the commercial name for the technology developed by the ZigBee Alliance. ZigBee transmits 10-75 meters, depending on the RF environment and the power output consumption required. It operates in the unlicensed RF worldwide (2.4GHz global, 915MHz Americas or 868 MHz Europe). The data rate is 250kbps at 2.4GHz, 40kbps at 915MHz and 20kbps at 868MHz.

3.1.2 MC1321x family

The MC1321x family is Freescales second-generation ZigBee platform which incorporates a low power 2.4 GHz radio frequency transceiver and an 8-bit microcontroller into a single 9x9x1 mm 71-pin LGA package. ¹ The radio is a short range, low power, 2.4GHz Industrial, Scientific and Medical (ISM) band transceiver designed to be IEEE 802.15.4 Standard compliant.

¹ For a detailed specification of the platform used in this experiment refer to Appendix A

3.1.3 The Link Quality Indicator (LQI)

The LQI measurement is a characterization of the strength and/or quality of a received packet. The measurement is implemented using the receiver detected energy, a signal-to-noise ratio estimation, or a combination of both methods. The LQI measurement is performed for each received packet, and the result is reported as an integer ranging from 0x00 to 0xff.

The minimum and maximum LQI values (0x00 and 0xff) are associated with the lowest and highest quality compliant signals detectable by the receiver. LQI values in between should be uniformly distributed between these two limits. In this thesis dBm units are employed and are calculated as $\text{dBm} = (-\text{Link Quality}/2)$, see [26]

The decibel (dB) is a logarithmic unit of measurement that expresses the magnitude of a physical quantity (in this case the power of the received signal) relative to a specified or implied reference level. Since it expresses a ratio of two quantities with the same unit, it is a dimensionless unit. A decibel is one tenth of a bel (B). In this thesis, "dBm" is employed. It indicates that the reference quantity is one milliwatt,

dBm (also written dBmW) is an abbreviation for the power ration in decibels (dB) of the measured power references to on milliwatt (mW). It is used in this thesis as a convenient measure of absolute power because of its capability to express both very large and very small values in a short form. The milliwatt is referenced to the watt, it is an absolute unit, used when measuring absolute power. By comparison, the decibel (dB) is a dimensionless unit, used for quantifying the ratio between two values, such as power emitted and power received. To express an arbitrary power P as x dBm, the following equation is used:

$$x = 10 \log_{10}(P) \quad (3.1)$$

When referring to measurements of power of the received signal, a ratio can be expressed in decibels by evaluating ten times the base-10 logarithm of the ratio of the measured quantity to the reference level. Thus, if L represents the ratio of a power value P_1 to another power value P_0 , then L_{dB} represents that ratio expressed in decibels and is calculated using the formula:

$$L_{dB} = 10 \log_{10}(P_1/P_0) \quad (3.2)$$

P_1 and P_0 must have the same dimension (in this work milliwatts), and must be converted to the same units before calculating the ratio of their numerical values. Note that if $P_1 = P_0$ in the equation 3.2, then $L_{dB} = 0$. If P_1 is greater than P_0 then L_{dB} is positive; if P_1 is less than P_0 then L_{dB} is negative. For illustrative examples of dBm values, see Table 3.1.

dBm level	Power	Notes
15 dBm	32 mW	Typical WiFi transmission power in laptops
10 dBm	10 mW	
6 dBm	4.0 mW	
5 dBm	3.2 mW	
4 dBm	2.5 mW	Bluetooth Class 2 radio, 10 m range
3 dBm	2.0 mW	More precisely 1.9952623 mW
2 dBm	1.6 mW	
1 dBm	1.3 mW	
0 dBm	1.0 mW=1000 μ W	Bluetooth Class 3 radio, 1 m range
-1 dBm	794 μ W	
-3 dBm	501 μ W	
-5 dBm	316 μ W	
-10 dBm	100 μ W	Typical maximum received power of wireless network
-20 dBm	10 μ W	
-30 dBm	1.0 μ W=1000nW	
-40 dBm	100nW	
-50 dBm	10nW	
-60 dBm	1.0nW=1000pW	
-70 dBm	100pW	Range of wireless (802.11x) received signal power

Table 3.1: This table summarize common cases of dBm values.[2]

The dBi, (isotropic decibel), is a unit of measurement of the antenna gain referenced to an ideal isotropic antenna. A negative number means that the antenna in question radiates less than the reference antenna and a positive number means that the antenna radiates more.

3.2 The experiment

3.2.1 The Design

The first step in this research was to perform a simple experiment to determine if it was reasonable to believe that the MC1319x short range transceiver could provide the signal strength data required for our algorithm. A zigbee network with only two sensor was formed in the middle of the Cinvestav soccer field and the experiment was setup as follows:

1. In the outdoor space, a sensor transmitter is placed at a central point and connected to a laptop running our measurement program. This sensor is called coordinator.
2. A second sensor is placed 1 meter away.
3. The second sensor is set in low power modes (LPM) and wake up every 5 seconds to send an identification number to the coordinator.
4. A 30 measurements sample is taken and logged.
5. The second sensor is moved to slightly increase (by 1 meter) the distance to the coordinator.
6. Step 4 and 5 are repeated until a 20 meters range is reached.
7. For all distances tested, the sensors are placed horizontal, and the antennas follow 4 different orientations.

The figure 3.1 shows the layout of the experiment in the Cinvestav soccer field.

3.2.2 The Data Collection & Analysis

A key step in this research is the data collection phase. The information of the LQI is recorded as a function of the distance of the second sensor. This information is used to construct and validate a model for the signal propagation as well as to explain the variability of the LQI measurements at certain distance.

A premise of this thesis is that the signal strength (RSSI) information provides a mean of inferring a distance. To demonstrate that this is a reasonable premise, Figure 3.2 presents experimental results of the RSSI measured at different points diminishes as the distance increases.

The dots in figure 3.2 represent only the mean. But, for each sample taken in step 4, we compute the mean, the standard deviation, and the median of the corresponding signal strength values for each distance (See Figure 3.3).



Figure 3.1: The transmitter and receiver sensors in the middle of the Cinvestav soccer field.

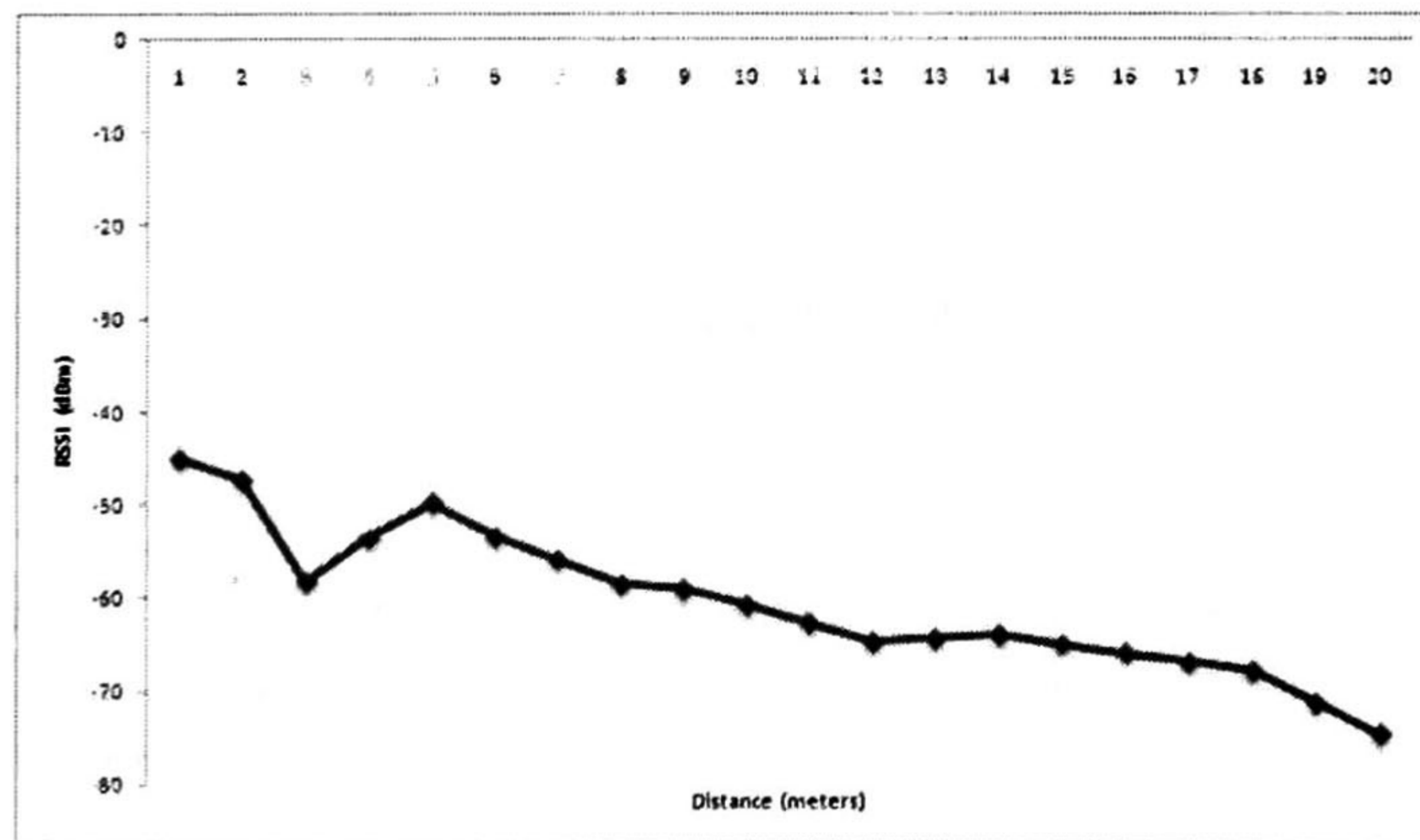


Figure 3.2: RSSI as a function of transmitter-receiver separation derived from the empirical data collected.

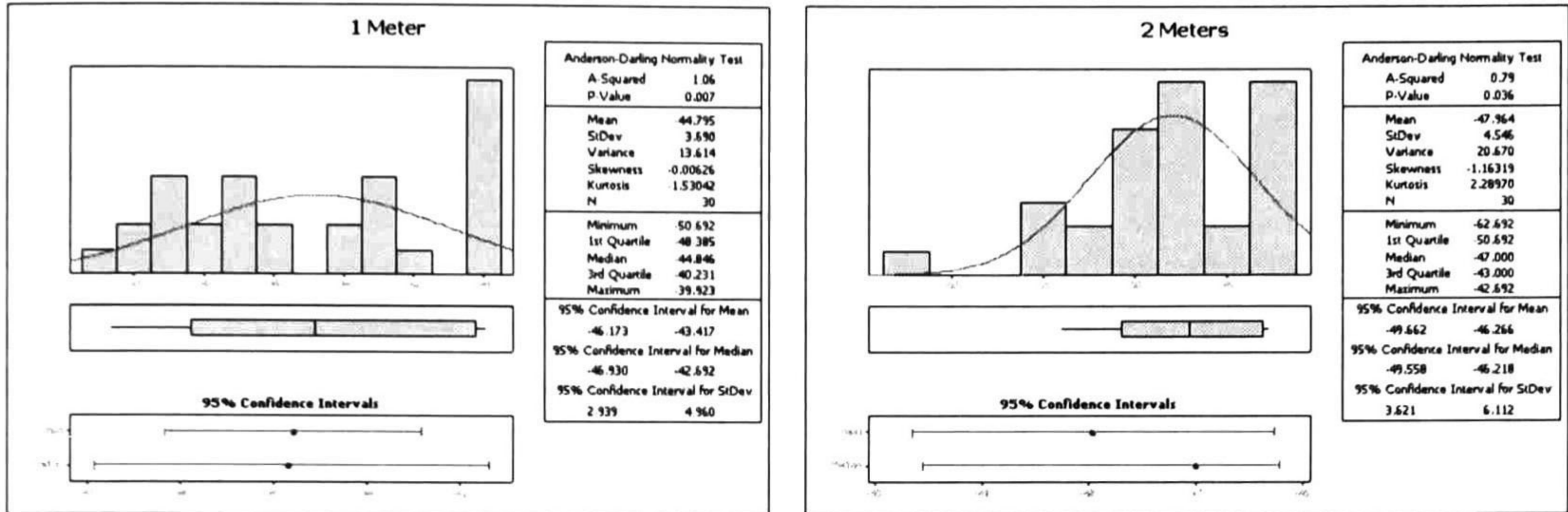


Figure 3.3: Mean, Standard Deviation and median for 1 and 2 meters of RSSI values.

From the experimental data it is observed a decreasing power results in a low RSSI measures. It means, distance d is indirect proportional to RSSI. In general, the RSSI-based algorithms use some signal propagation model that maps RSSI values to distance estimates (like the model presented in section 2.3.1).

The proposed model is based on **Friis free space transmission model** (equation 3.3). this model is ideal and RSSI decreases quadratically with the distance to the sender. It predict received RSSI when the transmitter and receiver have a clear, unobstructed line-of-sight path between them. It is classified as a *small-scale* or *fading* model, because characterize the rapid fluctuations or the received signal strength over short travel distance or short time durations.

$$P_r(d) = \frac{P_t G_t G_r (\lambda)^2}{(4\pi)^2 d^2 L} \quad (3.3)$$

P_t is the transmitted power, $P_r(d)$ is the received power which is a function of the distance, G_t is the transmitter antenna gain, G_r is the receiver antenna gain, d is the transmitter-receiver distance in meters, L is the system loss factor ($L \geq 1$), and λ is the wavelength in meters.

Figure 3.4 shows the free space propagation model versus distance, by using a unity gain in both antennas ($G_t = G_r = 1$), an applied power of 1 milliwatts ($P_t = 0.001$), and a 2.4 Ghz carrier frequency ($\lambda = 0.12$ meters).

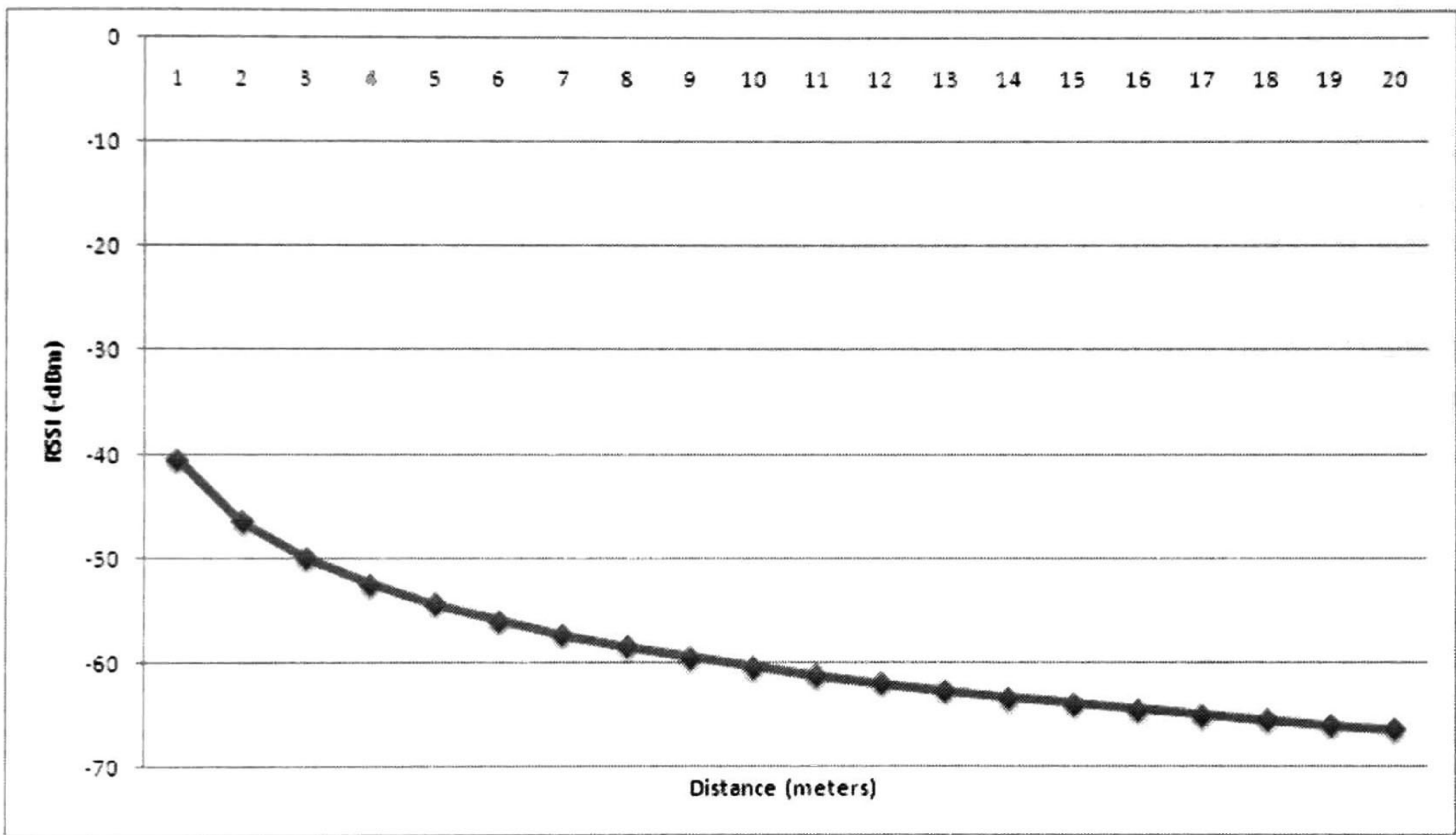


Figure 3.4: Free space propagation model plotting RSSI values versus distance (Friis Model)

However, in practical scenarios this model is not applicable because the propagation of the radio signal is interfered with several effects e.g.reflection on metallic objects, diffraction at edges,reflection on the ground, polarization of electromagnetic fields, etc. These effects degrade the quality of the RSSI significantly. Thus, the measurements present a very high variance.Other effects can also be present therefore statistical analysis is considered.

The proposed propagation model focus on predicting the averange RSSI at a given distance from the transmitter. Two important sources of variability of the signal strength are considered the **reflection on the ground** and the **antenna radiation pattern**.

3.3 The Lloyd Effect

A single electromagnetic signal can be diffracted into two signals, causing constructive and destructive interference to occur. **Interference** is the interaction of two or more signals yielding a resultant signal strength that deviates from the sum of the component signal strengths.

Lloyd's Mirror phenomenon consists of a flat surface of dielectric material (ground) which serves as a mirror from which one portion of the wave is reflected and the other portion proceeds directly to the screen, see Figure 3.5.

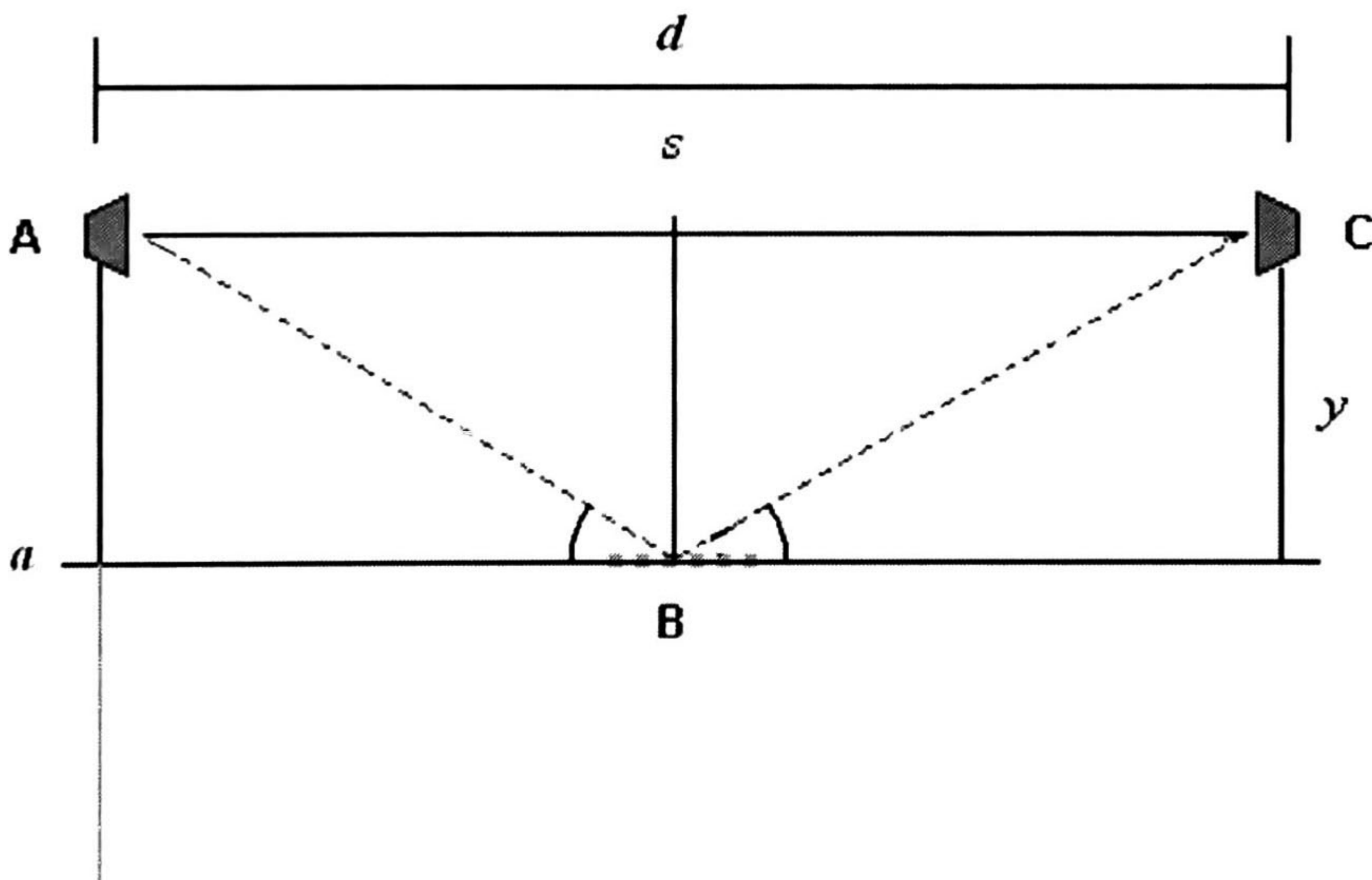


Figure 3.5: Lloyd's Mirror.

An electromagnetic signal from one source at point A is detected by a receiver at point

C. If radiation from A is reflected off a mirror at point B, the reflected wave will also be detected by the receiver. Due to the reflection from the mirror, the reflected wave will be 180° out of phase with respect to the incident wave. When the two waves meet at the receiver, constructive and destructive interference can occur. A maximum signal strength will be detected when the two waves reach the detector in phase. The optical path length of the reflected signal is defined as $AB+BC$. The optical path length of the un-reflected signal is just AC . The paths length δ vary as the transmitter and the receiver are moved away from each other.

For adding the signal strength from the two signal receivers at point C, it is necessary to use the Total Irradiance formula from optics, see equation 3.4.

$$I=I_1 + I_2 + 2\sqrt{I_1I_2} \cos \delta \quad (3.4)$$

Where I_1 is the signal strength received from the un-reflected signal, and I_2 is the signal strength received from the reflected signal. At different points in space, the resultant strength can be greater, less than, or equal to $I = I_1 + I_2$, depending on the value of $2\sqrt{I_1I_2} \cos \delta$.

A maximum signal strength is obtained when $\cos \delta = 1$. This happens when $\delta = 0, \pm 2\pi, \pm 4\pi$. So, $I_{max} = I_1 + I_2 + 2\sqrt{I_1I_2}$. This case is called **total constructive interference** because the phase difference between the two waves is an integer multiple of 2π , and the waves are in phase. When $0 < \cos \delta < 1$ the waves are out-of-phase, $I_1 + I_2 < I < I_{max}$, and the result is still a constructive interference.

At $\delta = \pi/2$, $\cos \delta = 0$, the waves are 90 degrees out of phase, and $I = I_1 + I_2$.

For $0 > \cos \delta > -1$ we have the condition of destructive interference, $I_1 + I_2 > I > I_{min}$. A minimum irradiance results when the waves are 180 degrees out of phase, troughs overlap crests, $\cos \delta = -1$, and $I_{min} = I_1 + I_2 - 2\sqrt{I_1I_2}$. This happens when $\delta = \pm\pi, \pm 3\pi, \pm 5\pi, \dots$, and is called **total destructive interference**. This angle is calculated from Transmitter-Receiver distance and heights as $\delta = (\frac{ay\pi}{s\lambda})$.

To illustrate the Lloyd Effect the following example is presented.

EXAMPLE.3.1 $P_t = 0.001$ (the transmitted power equal 1 milliwatt), G_t is the transmitter antenna gain, G_r is the receiver antenna gain, and both equal 1, $d = 1$ is the transmitter-receiver distance in meters, $y = 0.46$ meters (height of the transmitter and receiver from ground), L is the system loss factor and $L = 1$. Finally at 2.4 GHz frequency wavelength is $\lambda = 0.12$

Considering the Lloyd Effect, What is P_r (1 mts.)?.

Solution

First, from equation 3.4 we must calculate the signal strength from the un-reflected and reflected signals. So, $I_1 = P_r(AC) = 1\text{meter}$ and $I_2 = P_r(AB + BC) = 1.35882302\text{ meters}$.

Now, using equation 3.3:

A).

$$P_r(AC) = 0.001(1)(1)(0.12)^2 / (4\pi)^2(1)^2(1) = 9.118906529 \times 10^{-8} \text{ watts.}$$

B).

$$P_r(AB + BC) = 0.001(1)(1)(0.12)^2 / (4\pi)^2(1.35882302)^2(1) = 4.938749204 \times 10^{-8} \text{ watts.}$$

Now, we calculate angle δ .

$$\delta = (\pi)(0.2116)(.46) / (1)(0.12) = 11.07935009 \text{ rad.}$$

From equation 3.4

$$9.118906529 \times 10^{-8} + 4.938749204 \times 10^{-8} + 2\sqrt{4.503599236 \times 10^{-15}} \cos(11.07935009) = 1.518075582 \times 10^{-7} \text{ watts.}$$

We need to convert the signal strength from watts to dBm. so, first convert watts into milliwatts:

$$\frac{1.518075582 \times 10^{-7}}{0.001} = 1.518075582 \times 10^{-4} \text{ milliwatts}$$

Now, we use formula 3.1:

$$10 \log_{10}(1.518075582 \times 10^{-4}) = -38.18706605 \text{ dBm.}$$

In figure 3.6 we plot the free space propagation model versus distance but now considering the Lloyd Effect. Again a unity gain is used in both antennas ($G_t = G_r = 1$), an applied power of 1 milliwatts ($P_t = 0.001$), and a 2.4 GHz carrier frequency ($\lambda = 0.12$ meters).

Next, combining plots from Figures 3.2 and 3.6, the result showed in Figure 3.6 is obtained.

3.4 The antenna radiation pattern

In addition to Lloyd effect, the transmitting antenna characteristics significantly impact also the received average signal strength. This means that the RSSI value recorded at the receiver for a given pair of communicating nodes and distance varies as the antenna orientation of the transmitter and the receiver are changed.

The gain pattern of the F-antenna printed on the MC1321x family is shown in Figure 3.8.

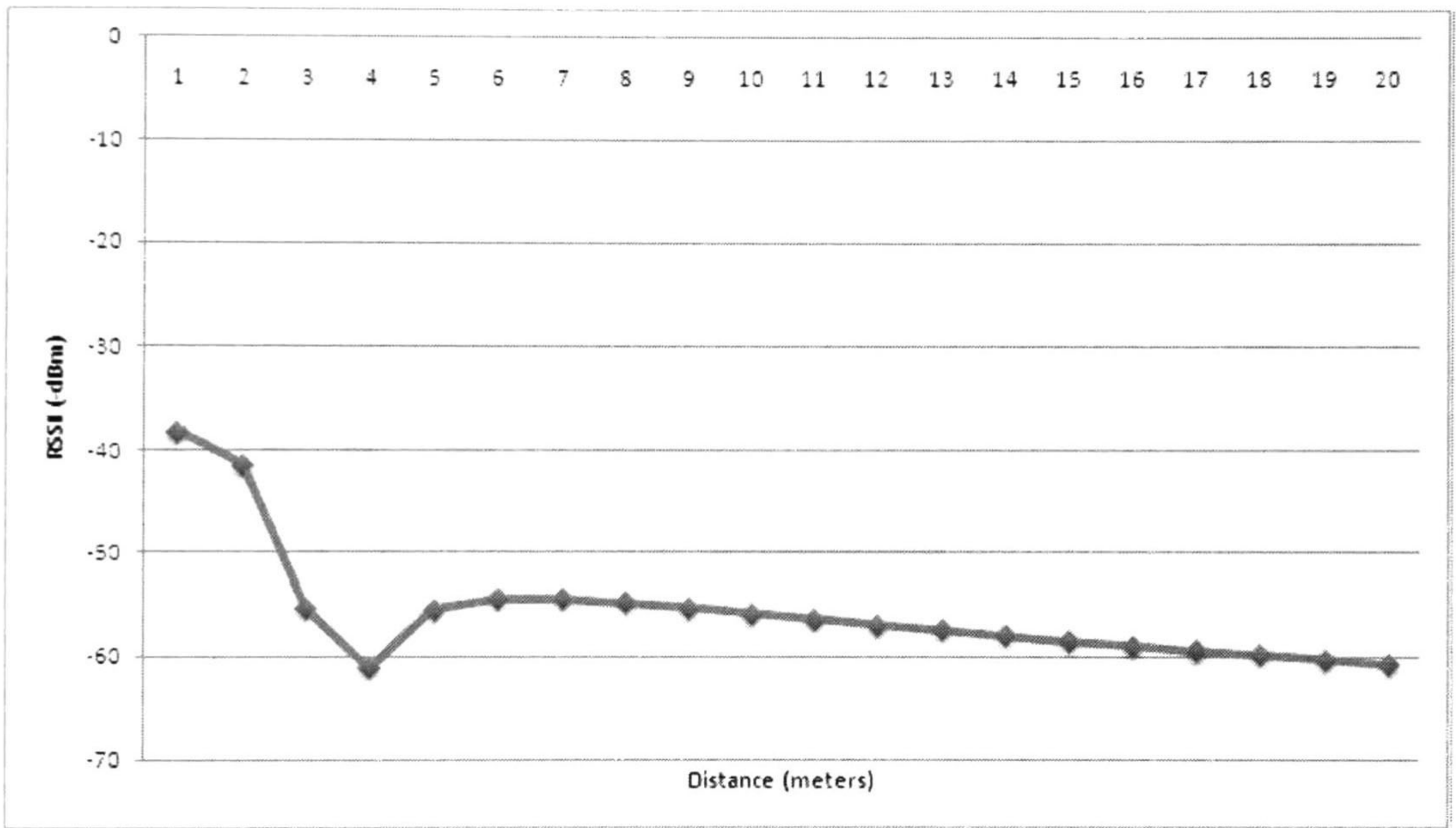


Figure 3.6: Lloyd Effect vs distance

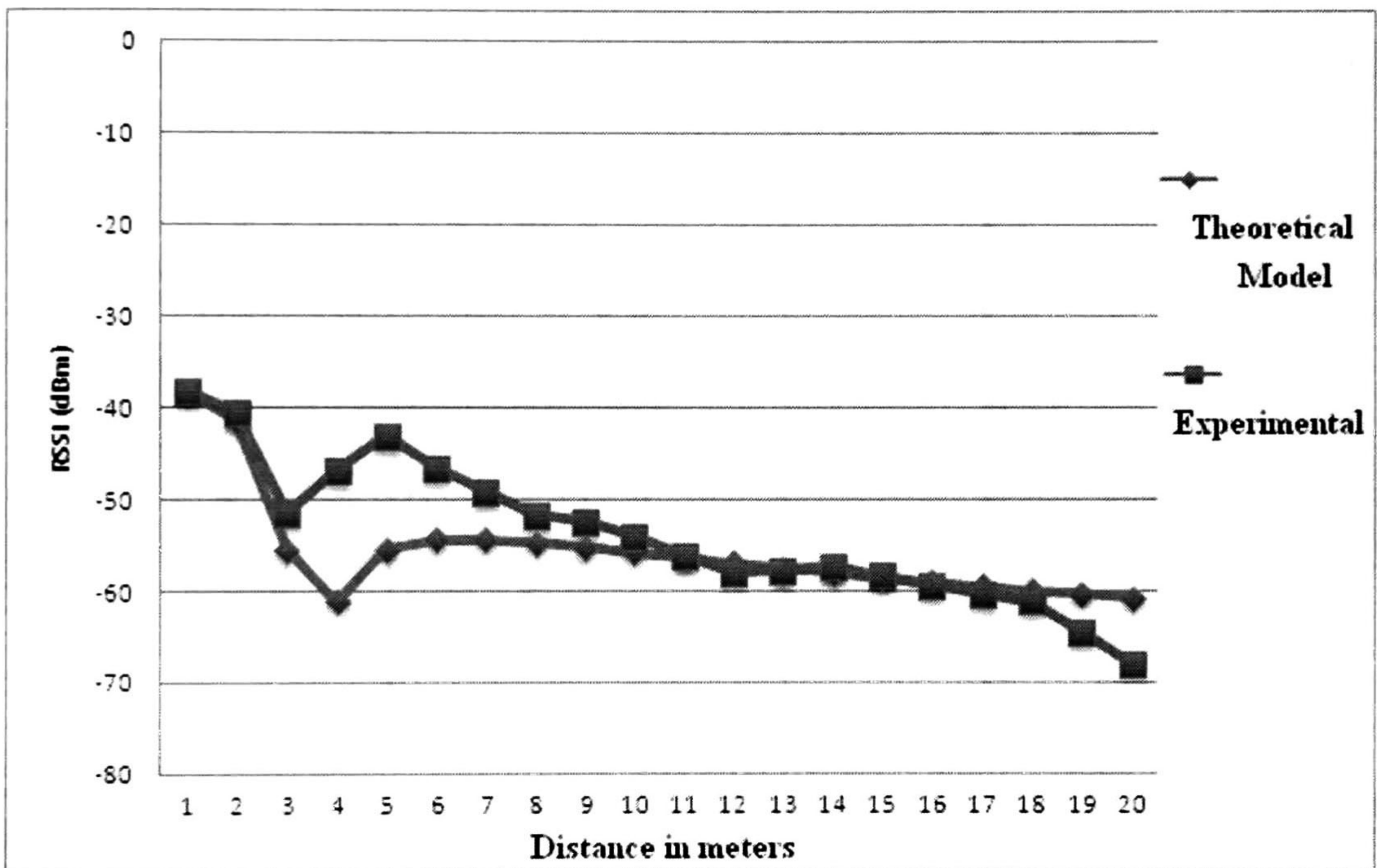


Figure 3.7: Theoretical Proposed model vs Experimental Data collected.

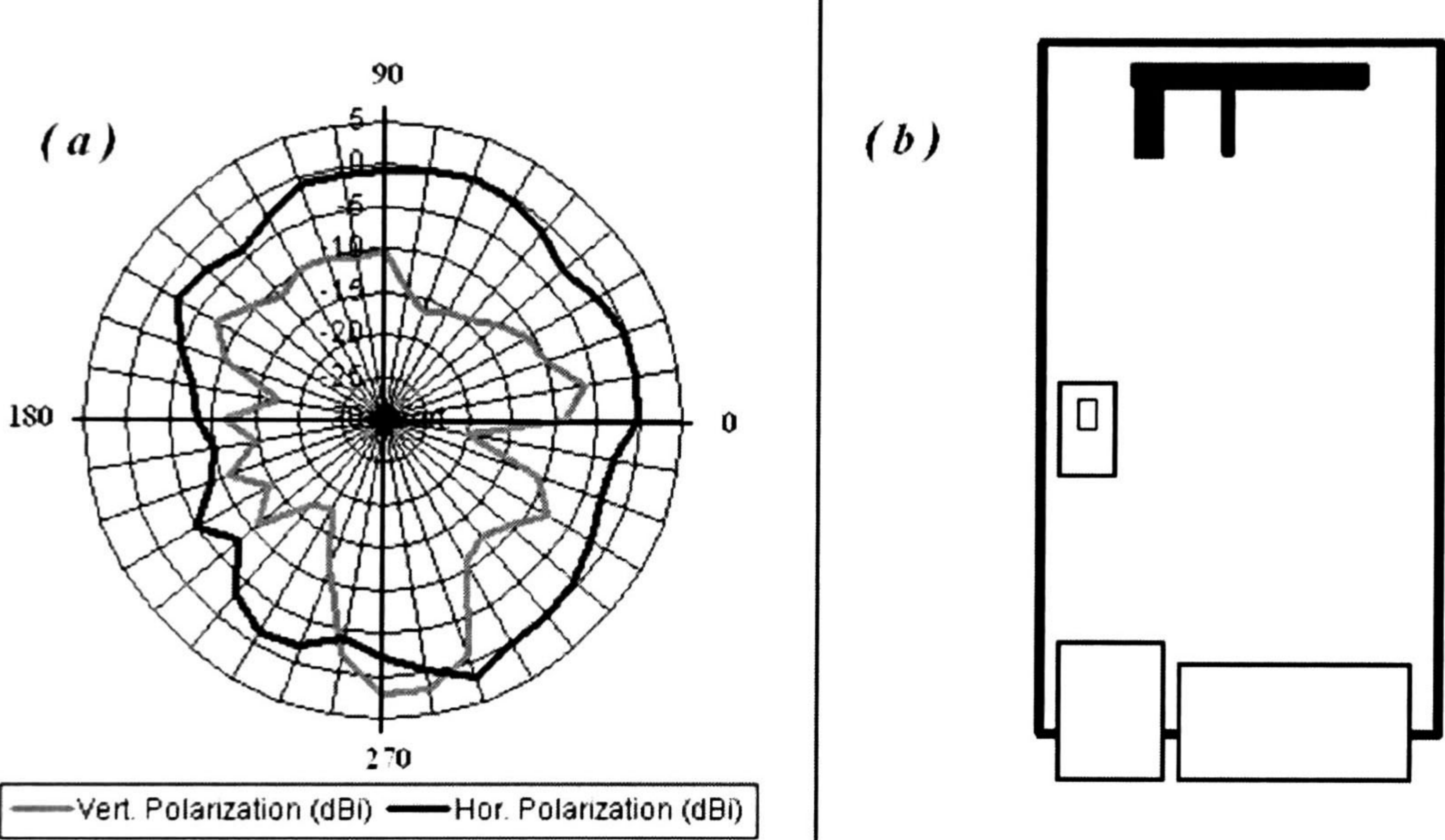


Figure 3.8: (a)Printed F-antenna Radation Pattern (b)Top view orientation of the MC1321x circuit board. Images taken from [3]

The top view of the board is shown to the right of the polar graph. The gains G_t and G_r depend on the orientation of the transmitter and receiver pattern, respectively. Experimental values of the antenna gains for 360 degrees are derived based on Figure 3.8(a) as shown in table 3.2.

As we cannot foresee the transmitter-receiver orientations, it is necessary to produce different outcomes of the received power at distances from 1 to 60 meters. This section is focused on the RSSI variation resulted for the antenna orientation. This variation is characterized by adding it to formula 3.4.

This is done by assuming that the receiver was exactly in the same position and with the same antenna orientation. The transmitter was placed at 1 meter far away and rotated for 37 different orientations (0,10,20,30,...360 degrees). For all orientations the average RSSI value and standard deviation were computed. The result for 1,2,3 and 4 meters are show in figures 3.9 and 3.10. All computed values are included in Appendix C.

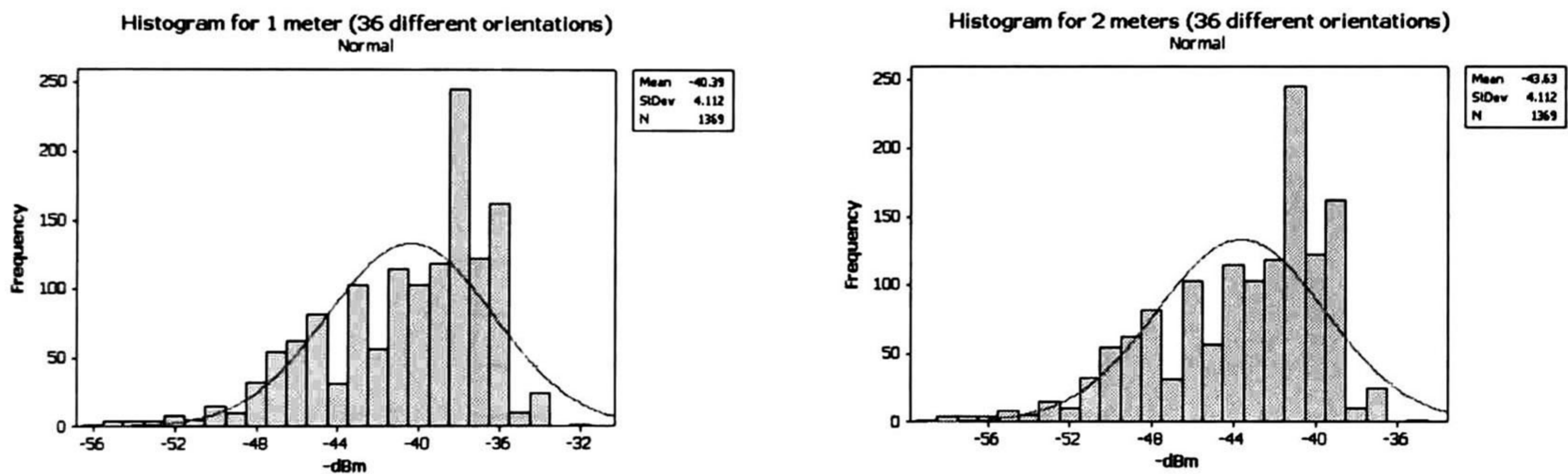


Figure 3.9: Transmitter placed 1 and 2 meters away from receiver. Receiver rotated 360 degrees.

The overall received RSSI values at 1,2,3 and 4 meters were -40.39, -43.63, -57.59, -63.38 dBm and the standard deviation value was -4.112 dBm considering different orientations. The obtained histogram for each experimental distance measurement is best fitted to a normal distribution based on these result and considering.

With the Friis free space transmission model (section 3.3.3), the Lloyd's effect (section 3.4) and the radiation pattern of the F-antenna (section 3.5) a model for the signal propagation is proposed as follows:

Degrees	dBi	Antenna Gain
0	0	1
10	0	1
20	0	1
30	-1	0.794328235
40	-2.5	0.562341325
50	-1	0.794328235
60	0	1
70	0	1
80	0	1
90	0	1
100	-1	0.794328235
110	-1	0.794328235
120	-2.5	0.562341325
130	-4	0.398107171
140	-2.5	0.562341325
150	-2	0.630957344
160	-5	0.316227766
170	-7	0.199526231
180	-9	0.125892541
190	-10	0.1
200	-9	0.125892541
210	-5	0.316227766
220	-7.5	0.177827941
230	-3.5	0.446683592
240	-1	0.794328235
250	-2	0.630957344
260	-4.5	0.354813389
270	-2.5	0.562341325
280	0	1
290	2	1.584893192
300	0	1
310	0	1
320	0	1
330	-2	0.630957344
340	-2.5	0.562341325
350	-2.5	0.562341325
360	0	1

Table 3.2: This table summarize the dBi values for 360 degrees

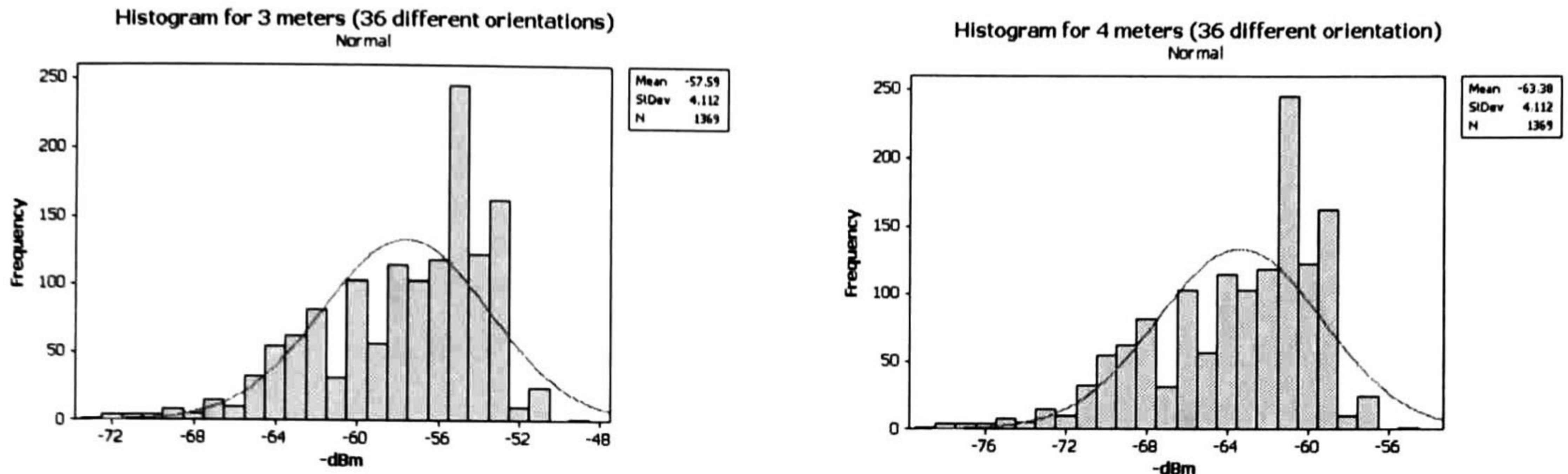


Figure 3.10: Transmitter placed 3 and 4 meters away from receiver. Receiver rotated 360 degrees.

$$RSSI_i \approx N(\mu, \sigma^2) \quad (3.5)$$

$RSSI_i$ is the resultant measurement, $\mu = P_{r1}(S_i) + P_{r2}(S_i) + 2\sqrt{P_{r1}(S_i)P_{r2}(S_i)} \cos(\frac{\alpha y \pi}{S_i \lambda})$, $\sigma^2 = -16.90dBm$ and S_i is the distance variable.

3.5 Conclusion

In this chapter the Zigbee protocol was presented. Also, the hardware platform used for the experiments was introduced.

An outdoor environment experiment to prove the premise that the signal strength (RSSI) could be used as an indicator to infer distance, was conducted. Friis's space propagation formula is used to describe the relation distance versus RSSI. The experimental results show that RSSI is a reasonable metric to estimate distance.

The results also show a ground reflection phenomenon that produces an interference in the signal. This phenomenon takes place when the receiver and transmitter are 1 to 4 meters away. The Lloyd's model describes this effect.

Based on these results a model is proposed to fit the obtained experimental data. This is based on both, Friis and Lloyd's model.

Chapter 4

Development of the proposed algorithm

4.1 Introduction

This algorithm is based on MDS. This is a technique from mathematical psychology that aims to display the structure of distance-like data (RSSI measurements) in a Euclidean space. This algorithm is a beaconless and produce a relative coordinate system which can be converted to a global coordinate system.

4.1.1 Zigbee Protocol Stack

The layer-2 of the OSI model (also called data link layer) transforms a raw transmission facility into a line that appears free of transmission errors to the upper layer (network). It accomplishes this task setting the data into data frames and transmit them sequentially. If the transmission is succesful, the receiver confirms correct receipt of each frame by sending back an acknowledgement frame.

Wireless Sensor Networks (like Broadcast networks) has an additional issue in the layer-2: how to control access to the shared channel. A special sublayer of this layer, the medium access control (MAC) sublayer, deals with this problem. In this thesis, the SMAC (Simple Mac) provided by the Freescale ´s implementation of Zigbee protocol to access the shared medium is used. The SMAC is a simple ANSI C based code stack available as sample source code. See [26].

Freescale ´s implementation of the Zigbee protocol is called *BeeKit Wireless Connectivity Toolkit*. It includes The SMAC. The *BeeKit Wireless Connectivity Toolkit* software architecture, and where SMAC is placed, is shown below.

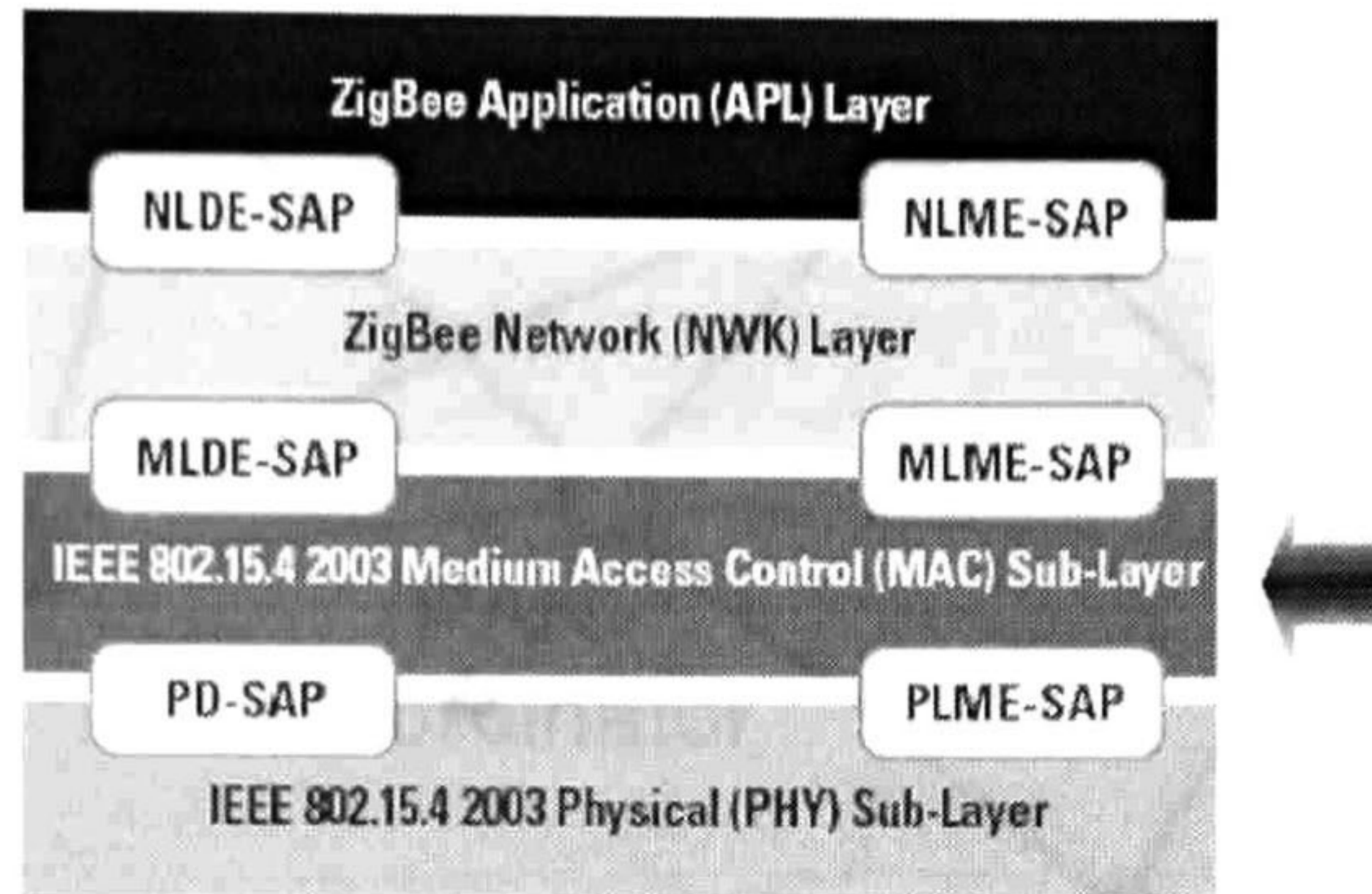


Figure 4.1: Zigbee Protocol Stack by Freescale.

There are two different device types within the Zigbee wireless sensor networks: full-function device (FFD) and reduced-function device (RFD). The FFD can operate in three modes as a personal area network **personal area network (PAN) coordinator**, a coordinator, or a device. An FFD can communicate to RFDs or other FFDs, while an RFD can communicate only to an FFD. An RFD is intended for extremely simple tasks. They do not have the need to send large amounts of data and may only associate with a single FFD at a time. Consequently, the RFD can be implemented using minimal resources and memory. For more detailed characteristic of the Zigbee technology see the standard [4].

4.1.2 Zigbee topologies

A zigbee wireless sensor network may operate in either of two topologies: *star* or *peer-to-peer*. In the star topology the communication is established between devices and a single central controller called the PAN coordinator. A PAN coordinator has associated an application that can be used to initiate, terminate or route the communication in the network. The PAN coordinator is the primary controller of the PAN.

The peer-to-peer topology has also a PAN coordinator, however, any device may communicate with any other ranging device without the coordinator. Peer-to-peer topology allows complex network formations to be implemented. See figure 4.2.

The experimental network topology was implemented as described in the following sections.

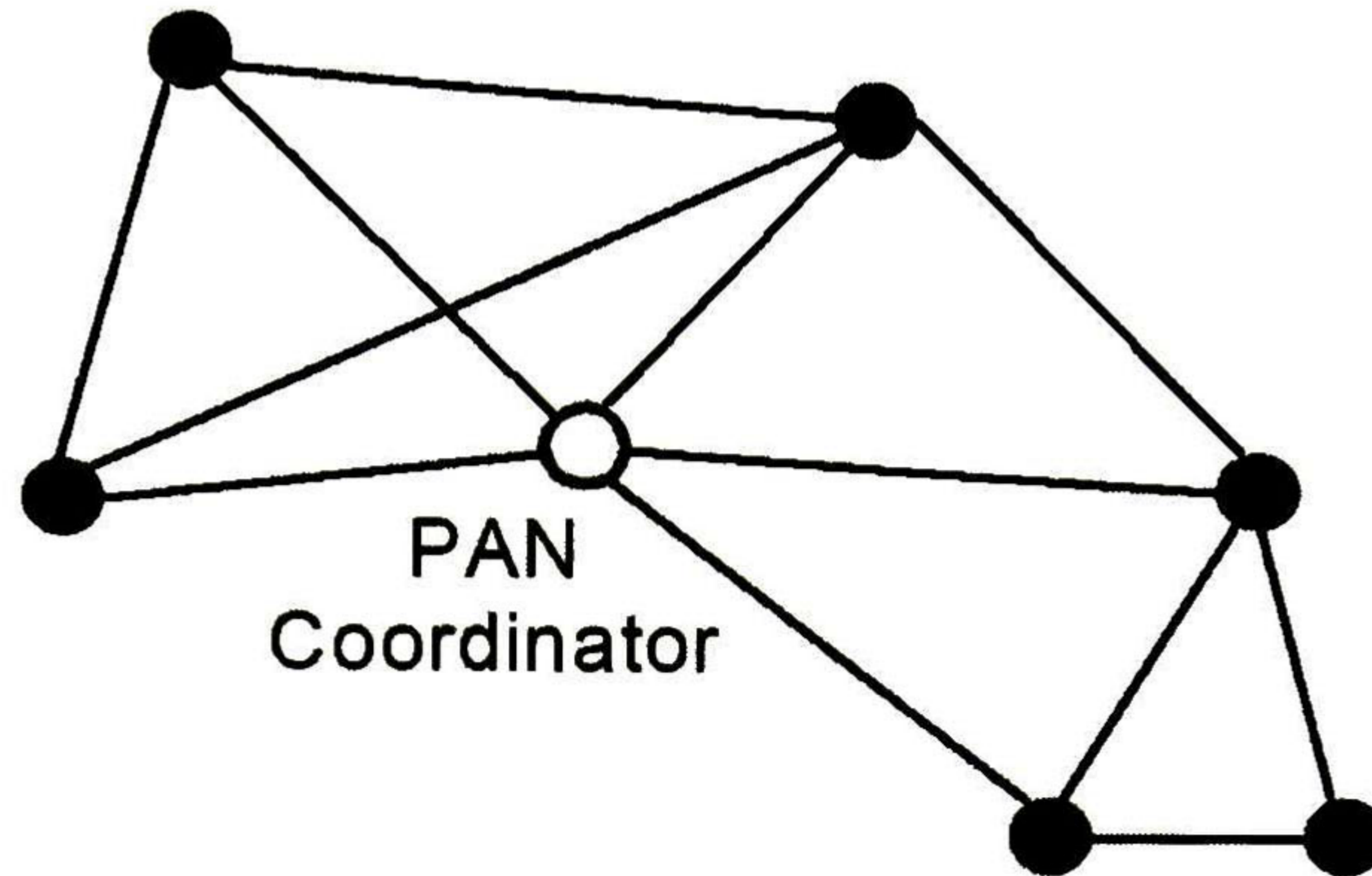


Figure 4.2: Peer-to-peer topology.

4.2 Experimental Network Implementation

1. N nodes are deployed.
2. The coverage area (clusters) are established and if configured a cluster tree is then formed.
3. To build a cluster tree network with information from step 2.
4. Each node samples RSSI from its neighbours based on the LQI packet field.
5. Each node sends a report with this information to coordinator.
6. The PAN coordinator estimates the distance between sensors using the reports.

The previous steps are described in detail next.

4.2.1 Nodes deployment

In WSN nodes are distributed in a randomly or in a deterministic way. In some cases nodes are able to change their location.

When distribution of all nodes is stochastic in the deployment phase, an estimation of the nodes position is required.

4.2.2 Building the network topology

In the peer-to-peer topology each device is able to communicating with any other within its coverage area. The PAN coordinator is the primary controller of the network. It forms a

cluster by choosing an unused PAN identifier and broadcast beacon frames to the neighbor devices. A neighbor receiving a beacon frame may request to join the network to the PAN coordinator. If the request is accepted the PAN coordinator adds the new device to its neighbor list. The newly joined device adds the PAN coordinator in its neighbor list and begins transmitting periodic beacons. Any node can join more than one coordinator at anytime.

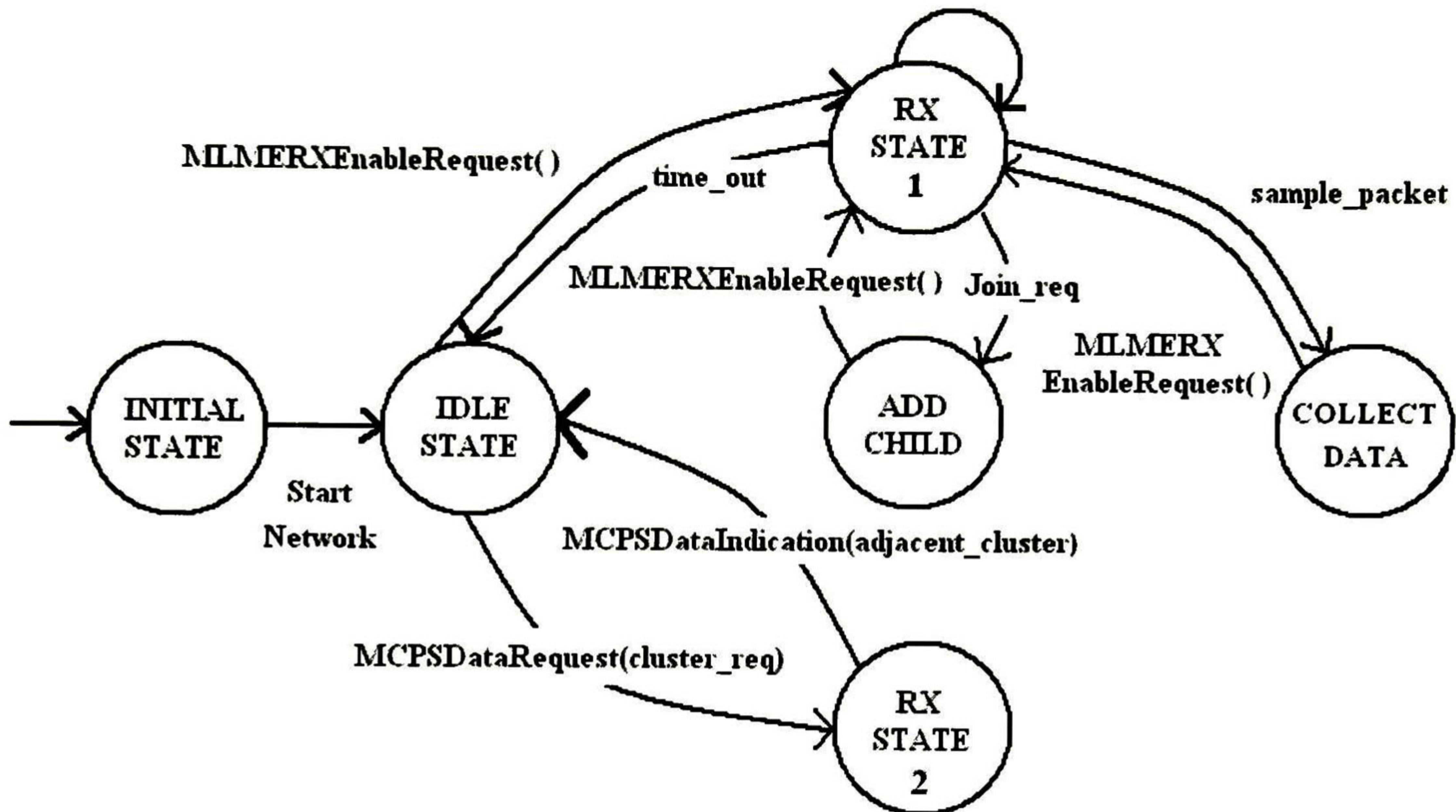


Figure 4.3: The state diagram for PAN Coordinators

The state diagram that describe the PAN coordinator behavior is shown in Figures 4.3. The state and transitions are described next:

TRANSITIONS

- **MLMERXEnableRequest:** places the radio into receive mode on the channel.
- **Start Network:** sets a channel for the zigbee protocol and set an ID for the Network. Finally go idle.
- **MCPSPDataIndication:** this is a function that is placed within the application code and is needed by the SMAC. This allows the SMAC to call this function when data is received by the radio to be processed by the application.
- **MCPSPDataRequest:** This function is used to send a packet.

- `MCPSPDataRequest(cluster req)`: Sends a broadcast packet that can be received for others PAN coordinators..
- `MCPSPDataIndication(adjacent cluster)`: a packet is recived from other PAN coordinator..
- `Join req`: a sensor neighbor device asked to join the PAN coordinator..
- `sample packet`: a packet with RSSI information has been received.
- `time out`: no packet from the sensor has been received.

STATES:

- `INITIAL STATE`: turns on the circuit.
- `IDLE STATE`: waits if no sensor sends packets.
- `RX STATE 1`: the radio is in receive mode, but only for a neighbor device.
- `RX STATE 2`: the radio is in receive mode, but only for other PAN coordinators.
- `ADD CHILD`: the PAN coordinator accepts a neighbor device which asks to joint the network.
- `COLLECT DATA`: the RSSI information from sensors packts is logged in the specific sensor file.

4.2.3 RSSI Reports

As mentioned before, there are two different device types: full-function device (FFD) and reduced-function device (RFD).

The sensors in the experimental WSN are FFD which operate as devices. This allows them to sample the RSSI from its neighbors. The following state diagram shows how this is preformed.

The state diagram that describe the neighbor devices behavior is shown in Figures 4.4. The state and the transitions are described next:

TRANSITIONS

- `request join`: requests to joint a network available within the coverage area.
- `MCPSPDataIndication(sample req)`: a neighbor device asks for a 30 packet sample.
- `sample complete`: the sensor sends a sample and return to idle state.
- `MCPSPDataRequest(sample req)`: the sensor asks to some neighbor device for a sample.

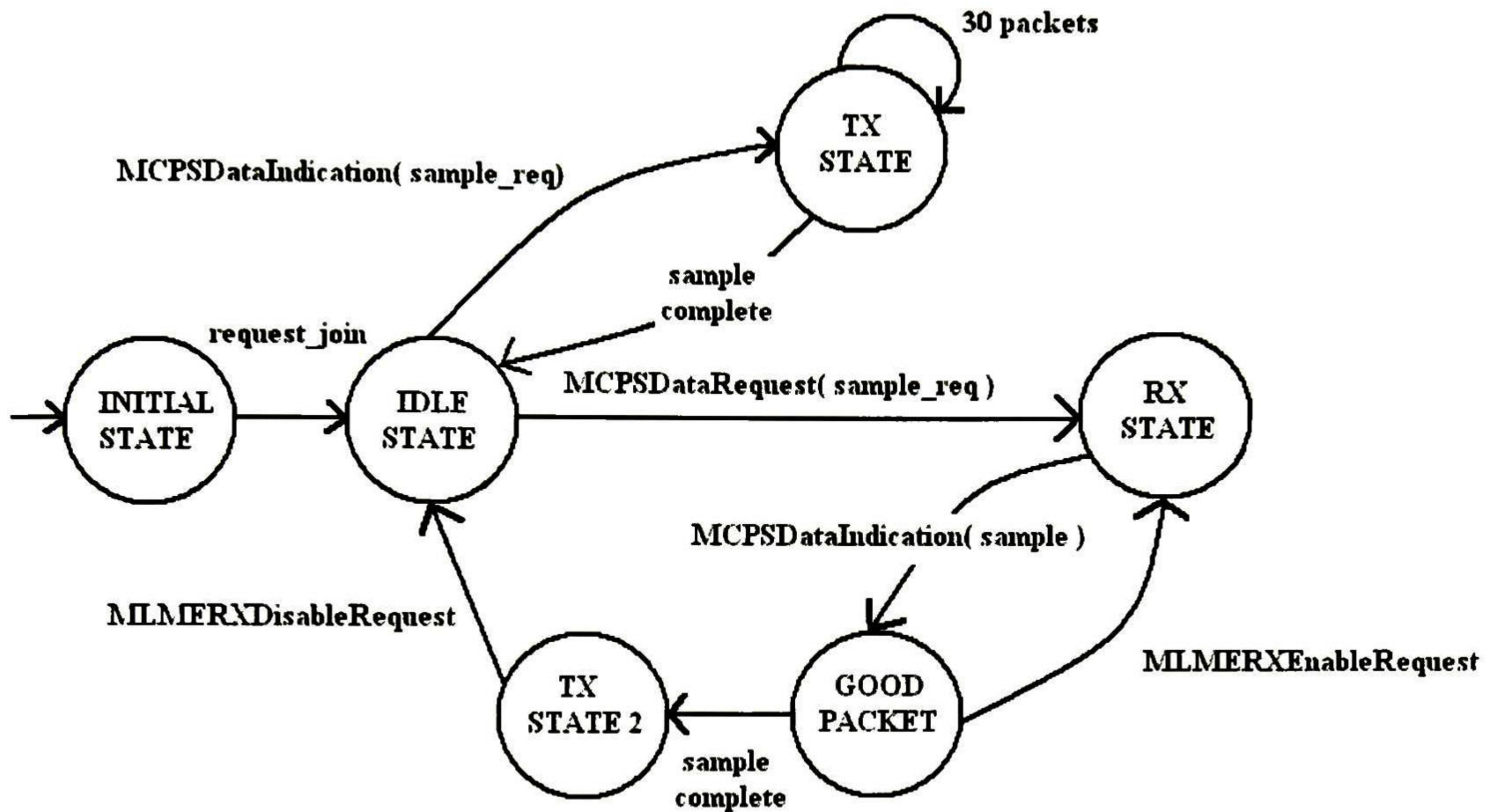


Figure 4.4: The state diagram for neighbor devices (sensors)

- **MLMERXEnableRequest**: places the radio into receive mode on the channel.
- **MLMERXDisableRequest**: disables the radio.
- **MCPSDataIndication(sample)**: a packet from a sample is received.

STATES:

- **INITIAL STATE**: turns on the circuit.
- **IDLE STATE**: waits if no packets are received.
- **TX STATE 1**: sends 30 packets with RSSI information.
- **TX STATE 2**: sends the mean and StDev of one sample to its PAN coordinator.
- **RX PACKET**: receives packets from other devices.
- **GOOD PACKET**: completes a report from some neighbor device

To form bigger networks to cover a larger area is possible by forming a mesh of multiple neighboring clusters, this is exclusively managed by the PAN coordinators. Seen Figure 4.4.

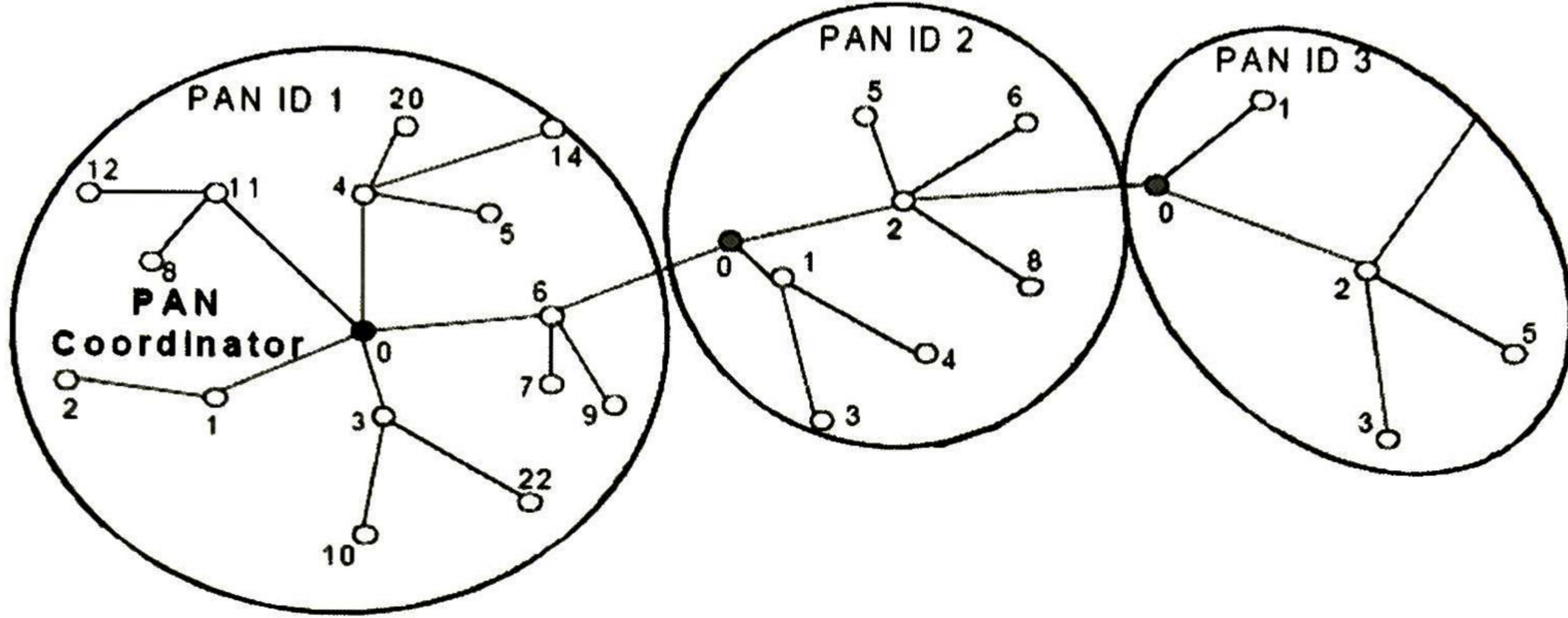


Figure 4.5: A cluster tree with 3 PAN id. Image taken from [4]

4.2.4 The PAN coordinator estimates distances between sensors.

In order to test real data obtained by sensors against the model proposed, statistical techniques are needed. The estimation theory provide tools such as *the hypothesis testing*. *Hypotesis testing* is a mechanism which help to obtain the best estimation of distance from the RSSI information provided by the reports.

To estimate distance from the reports (samples) sent by the sensors, an hypothesis about RSSI population parameters value at a given distance is required. As discused in section 3.5 at a given distance different RSSI values may be obtained. This variability is caused by the Lloyd effect, radiation pattern of the antenna, and other factors. From the theoretical model provided in section 3.6. the mean of the RSSI values at each considered distance is known along with the overall $\sigma = 2.947dBm$

For example, consider the theoretical values and the overall testing for hypotesis the mean and variance of the population of RSSI values at 1 meter of distance. The null hypothesis is formulated as follows: $H_o = -38.002dBm$. It basically states that there is no difference in RSSI between the sample and that theoretical values at 1 meter away. Next the null hypothesis is tested using the collected data. The sample: -38, -39, -38, -38, -39, -38, -38, -38, -39, -39, -39, -38, -38, -38, -39, -38, -38, -38, -38, -38, -39, -39, -39, -38, -39, -38, -38 and -39 dBm.

1. $H_o = -38.002dBm$

2. $H_1 \neq -38.002dBm$

3. $\alpha = 0.05$

4. Critical region: $z < -1.96$ and $z > 1.96$

5. With $\bar{x} = -38.4dBm$ and $n = 30$

$$z = \frac{-38.4 - (-38.002)}{2.947/\sqrt{30}} = -0.74$$

The sample mean \bar{x} lies inside the interval $(-z_{\alpha/2}, z_{\alpha/2})$, and we should accept H_0 with 95% confidence. Thus, a 1 meter distance to the sensor which collected the above sample is assigned. The following algorithm for hypothesis testing is proposed.

```

1 FUNCTION test_hypothesis(distance,sample_mean,sample_quantity,significance_level)
2 FOR d=1 TO 60 DO
3   SET H0=d_mean
4   SET H1!=d_mean
5   low_limit=GAUSS(-z,significance_level)
6   high_limit=GAUSS(+z,significance_level)
7   SET z=(sample_mean-d_mean)/(d_StDev/sqrt(sample_quantity))
8   IF (low_limit <= Z => high_limit)
9     SET distance=d
10    RETURN distance
11    BREAK
12  END
13 END
14 END

```

The PAN coordinator estimates a distance between each pair of its sensors using the algorithm. This is the first step to construct an embedding of the nodes in a plane by assigning coordinates to them. Next step is the MDS analysis. This is described in the next section.

4.3 The Localisation Algorithm

4.3.1 General description

The algorithm is based on multidimensional scaling (MDS). It is a data analysis technique from mathematical psychology, invented by Torgeson in 1952 who gave the preliminary ideas [16]. Since then many researchers have developed different varieties of MDS like nonmetric MDS, weighted MDS, qualitative MDS, iterative MDS etc. This data analysis technique aims to display the structure of distance-like data in a Euclidean space.

Basically MDS transforms a distance matrix in a set of coordinates such that the (Euclidean) distances derived from these coordinates approximate as much as possible the real distances of the sensors. The basic principle consists in transforming a distance matrix into a cross-product matrix in order to find its eigen-descomposition using Singular Value Decomposition (SVD) ² [27]. This techniques was applied to the localisation problem in [17] by Shang et al. It can be summarised as follows:

$$A(\text{Conectivities}) \rightarrow D = M_{n \times n}(\text{Distances}) \rightarrow B = M_{n \times n}(\text{CrossProduct}) \rightarrow SVD \rightarrow X = (\text{coordinates}, x_1, x_2, x_n)$$

Each steps is described in detail in the following sections.

4.3.2 Graph Matrix ($A(\text{Conectivities})$)

The connection among neighbour child sensors nodes and the physical distance between them is estimated from the RSSI measurements as we saw in last section. These connections are represented as an undirected graph (G) by using a adjacency matrix, $A(G) = [a_{ij}]$, in wich a_{ij} is associated with the estimated distance between sensors i and j . Note that this is not the number of edges joining the nodes.

4.3.3 Distance Matrix ($D = M_{n \times n}(\text{Distances})$)

Based on this adjacency matrix a second (distance) matrix is generated to represent the shortest path distances between all pair nodes. Here the well-known Floyd-Warshall algorithm is used. The *all-pairs shortest-paths* algorithm finds a shortest path from u to v for every pair of vertices u and v .

4.3.4 Cross Product Matrix ($B = M_{n \times n}(\text{CrossProduct})$)

Once the distance matrix, $D = M_{n \times n}$ is obtained from Floyd-Warshall algorithm, it is necessary verify that D holds with 3 axioms of Euclidian distance.

$$d_{ij} = 0 = d_{ij} \text{ (No negativity)}$$

$$d_{ij} = d_{ji} \text{ (Symmetry)}$$

$$d_{ij} = d_{ik} + d_{kj} \text{ (Triangular inequality)}$$

The first two axioms are meet easily, because RSSI samples do not infer negative distances. In order to meet the third axiom the minimum value of an additive constant C is calculated.

² Refer to Appendix B for more detail on SVD

This is done as follows:

For all the sub-indices in the matrix calculate

$$1) C_{min} = \max_{(i,j,k)} \{d_{ij} - d_{ik} - d_{kj}\}$$

Add C to all elements of the matrix.

2) Next we convert D into a matrix of dot products of vectors by applying the following operations:

$$B_{n \times n} = M_{n \times n} \text{ where } b_{ij} = -1/2(d_{ij}^2 - d_{i*}^2 - d_{*j}^2 + d_{**}^2)$$

$$d_{i*}^2 = 1/n \sum_{j=1}^n d_{ij}^2 \text{ (mean quadratic distance per row)}$$

$$d_{*j}^2 = 1/n \sum_{i=1}^n d_{ij}^2 \text{ (mean quadratic distance per column)}$$

$$d_{**}^2 = 1/n^2 \sum_{i=1}^n \sum_{j=1}^n d_{ij}^2 \text{ (mean quadratic distance of the matrix)}$$

4.3.5 Singular value decomposition (SVD)

Finally apply SVD to B to obtain the eigen-decomposition $B = UVU^T$. To obtain the coordinates matrix $X = M_{n \times n}$ we compute $X = UV^{1/2}$. As we want to get the 2 dimension of the solution, we denote the matrix of largest 2 eigenvalues by V_i and U_i the first 2 columns of U . Then, the coordinate matrix is $X_i = U_i V_i^{1/2}$.

```

1 FUNCTION mds(distance_matrix,coordinate_matrix)
2   DECLARE temporal_matrix
3   DECLARE V_matrix
5   DECLARE Work_matrix
6   DECLARE S_vector
7   DECLARE sigma vector
8   FOR i=1 TO num_row
9     FOR j=1 TO num_col
10      SET sum=0
11      SET mij=0
12      FOR k=0 TO num_row
13        SET mij=distance_matrix[i,k]
14        SET sum=sum+POW(mij,2)
15      END
16      SET d2i=sum/num_row
17      SET sum=0
18      SET mij=0
19      FOR l=0 TO num_col
```

```

20     SET mij=distance_matrix[l,j]
21     SET sum=sum+POW(mij,2)
22     END
23     SET d2j=sum/num_col
24     SET sum=0
25     SET mij=0
26     FOR k=1 TO num_row
27         FOR l=1 TO num_col
28             SET mij=distance_matrix[k,l]
29             SET sum=sum+POW(mij,2)
30         END
31     END
32     d2=sum/(num_row*num_col)
33     mij=distance_matrix[i,j]
34     temporal_matrix[i,j]=(POW(mij,2)-d2i,d2j-d2)/2
35     END
36     END
37
38     GSL_LINALG_SV_DECOMP(temporal_matrix,V_matrix,S_vector,Work_matrix)
39
40     SET eigen_value_1=SQRT(S_vector[0])
41     SET eigen_value_2=SQRT(S_vector[1])
42     FOR j=1 TO num_row
43         SET coordinate_matrix[j,0]=temporal_matrix[j,0]*eigen_value_1
44         SET coordinate_matrix[j,1]=temporal_matrix[j,1]*eigen_value_2
45     END
46     END

```

4.4 Conclusion

In this chapter the localisation of nodes in a coordinate system has been approached using MDS. MDS was used to obtain a 2-D relative map, but an absolute map can be obtained too. The task of finding an absolute map is to determine the absolute geographic coordinates of all the nodes and will depend on the number of beacons nodes availables.

A methodology for the sensor network formation was proposed and tested. In addition to this methodology, a simple protocol that collects the data to estimate distance from RSSI was presented.

The distances between sensors were from RSSI measurement using tools from estimation theory. In particular the hypothesis testing procedure with a 95% confidence level was employed to test sensors reports against the theoretic model.

Chapter 5

Experimental Results

5.1 Introduction

In section 2.2 it was discussed that in a Wireless Sensor Network a node can be one of two kinds: a **Beacon** or **Unknown**. The beacon nodes are nodes which coordinates are known *a priori*. The coordinates can be hard coded or obtained through some additional hardware such as a GPS. Beacon nodes (also called anchor nodes) are a prerequisite for localization in some algorithms such as RADAR, SpotON or Overlapping Coverage Areas. Other algorithms use beacons to "bootstrap" the positions of the unknown nodes.

This chapter is divided into two sections. The first section (5.3) shows the results of the algorithm when using beacon nodes. In the second section (5.4) the results without using beacon nodes are presented. In each section a comparison is made between simulations and real experimental results. For this random dBm measurements are generated based in the proposed model in section 3.6. Then the localisation algorithm is applied with these data. In a second phase, real dBm measurements are collected under outdoor environmental conditions environment and also fed into the algorithm.

5.2 The localisation algorithm under the use of beacons

The experimental testbed was located at the Cinvestav football pitch. It has dimension of 62 m by 25 m. (an area of 1,550 sq. m.). 8 beacon sensors were placed at every 20 m from each other in all directions. The experimental area was 60 m by 20 m. (1200 sq.m.) The layout of the field is shown in the Figure 5.1.

A cartesian coordinate system with origin (point 0,0) is centered in the middle of the field. Any node can be located by using this coordinate system. The 8 beacon nodes (square) are set

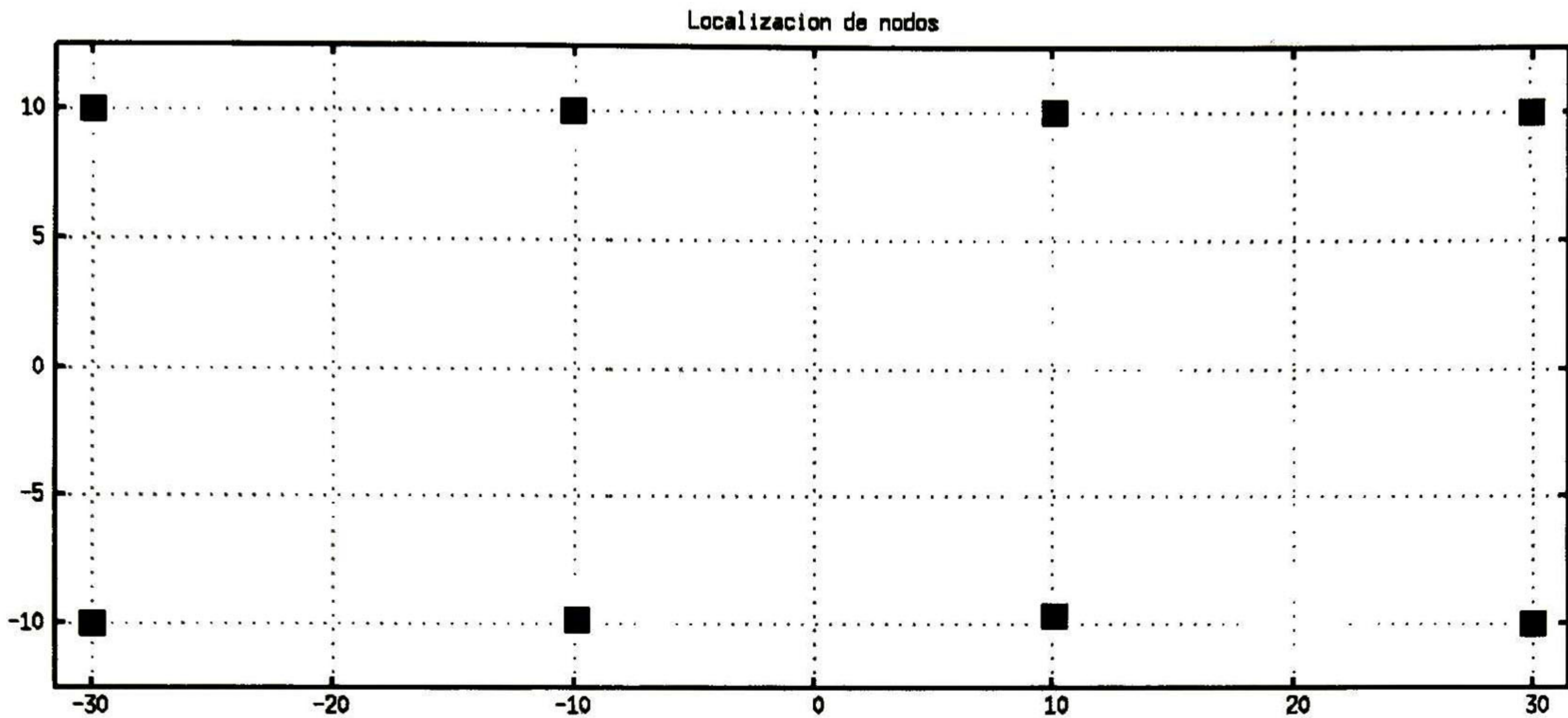


Figure 5.1: 8 beacon sensors layout

in Low Power Mode (LPM) and awake every 5 seconds to send a packet with its identification number and its position in the football pitch.

A 9th (unknown location) sensor is randomly placed in the football pitch area (triangle). This sensor is always awake and receives the packets coming from the beacons. The sensor calculates the RSSI of the received packets and sends it to a gateway. This sensor is connected to a computer running linux minicom. The sent packet includes an identification number of the beacon and the calculated RSSI. The identification numbers are 1,2...8.

The precision is measured using the Euclidian distance formula. This is $d(P_1, P_2) = \sqrt{(x_2 - x_1)^2 + (y_2 - y_1)^2}$ where P_1 and P_2 are the estimated and physical location respectively. The *error on x-axis* is defined as the difference $x_2 - x_1$ and the *error on y-axis* as $y_2 - y_1$.

5.2.1 Simulation

A simulation was performed using random dBm measurements given a certain position for the unknown node and a distance to the beacon nodes. To generate the random measurements the formula 3.4 (section 3.4) was applied by varying the transmitter antenna output power, the gains of transmitter-receiver, and the distance to the beacon node. This position was chosen randomly according to the layout of the football pitch. For example in Figure 5.2 the unknown node is placed in position X=15.0 Y=5.0 (this sensor is represented with a triangle and different estimated positions with black X's).

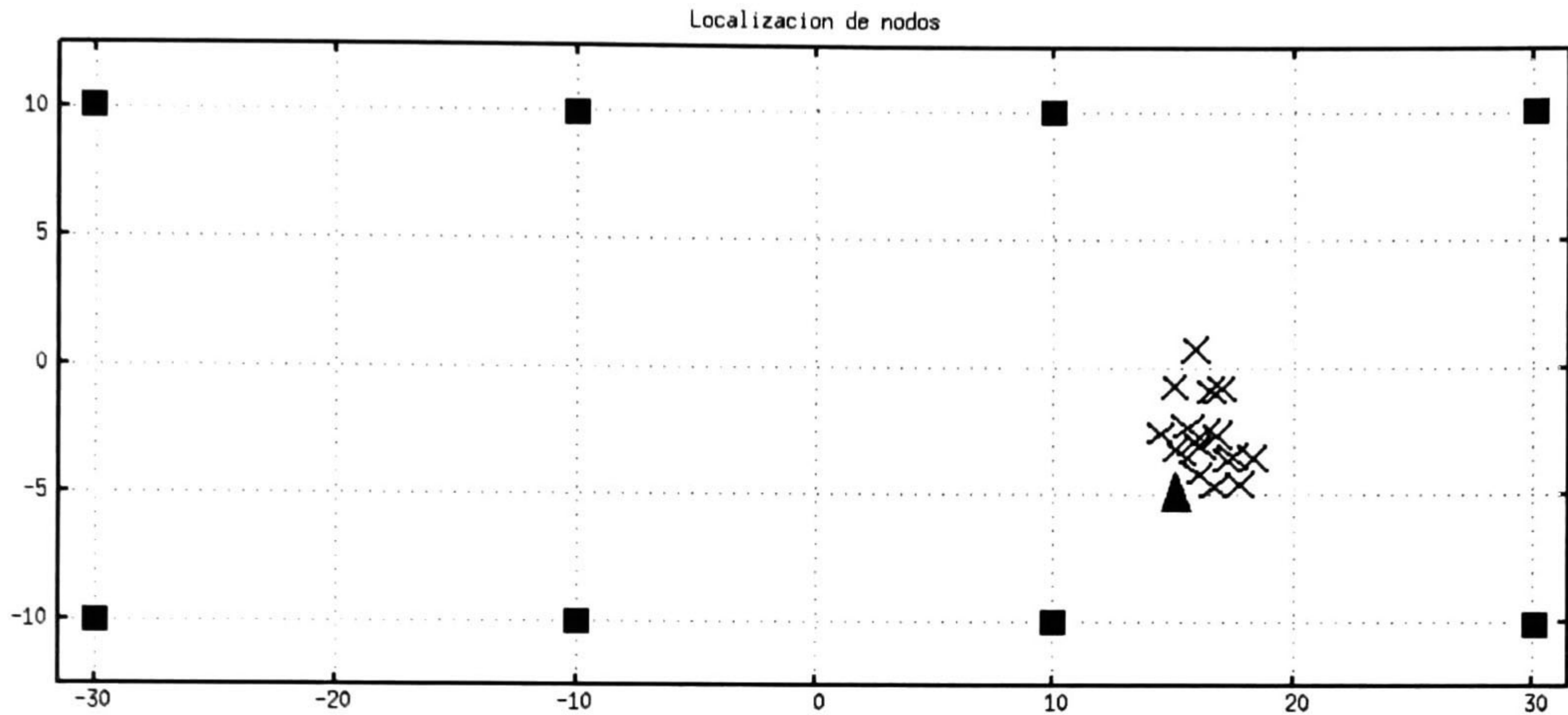


Figure 5.2: Different estimations for one random position

The simulation was run 1,000 times and logged into a log file. Using this data the *error distance* is calculated for both on the *error on the x-axis* and *y-axis*. The results are shown in figure 5.3.

The *error distance* the mean was 2.4951 mts and the standard deviation was 0.4546 mts. The minimum error was 0.9263 mts and the maximum error was 5.5512 mts. For the *error on the x-axis* the mean was 1.2198 mts and the standard deviation was 0.8757 mts. The minimum error was 0.1379 mts and the maximum error was 3.3293 mts. For the *the error on the y-axis* the mean was 2.0024 mts and the standard deviation was 0.4105 mts. The minimum error was 0.4007 mts and the maximum error was 5.3349 mts.

5.2.2 Field Experimental Work

Following the described experimental scenario 8 different random positions were tested under real outdoor conditions. The results are shown in the following sections.

The unknown sensor was placed at each position shown in Table 5.1 inside the Cartesian plane shown in Figure 5.2, then the algorithm was executed and the results are shown in Table 5.2. These results can also be seen from Figure 5.4 to Figure 5.11 (triangle represents the unknown sensor, squares represents the beacon nodes and X represent the estimation).

The table 5.1 summarizes the errors for all considered positions.

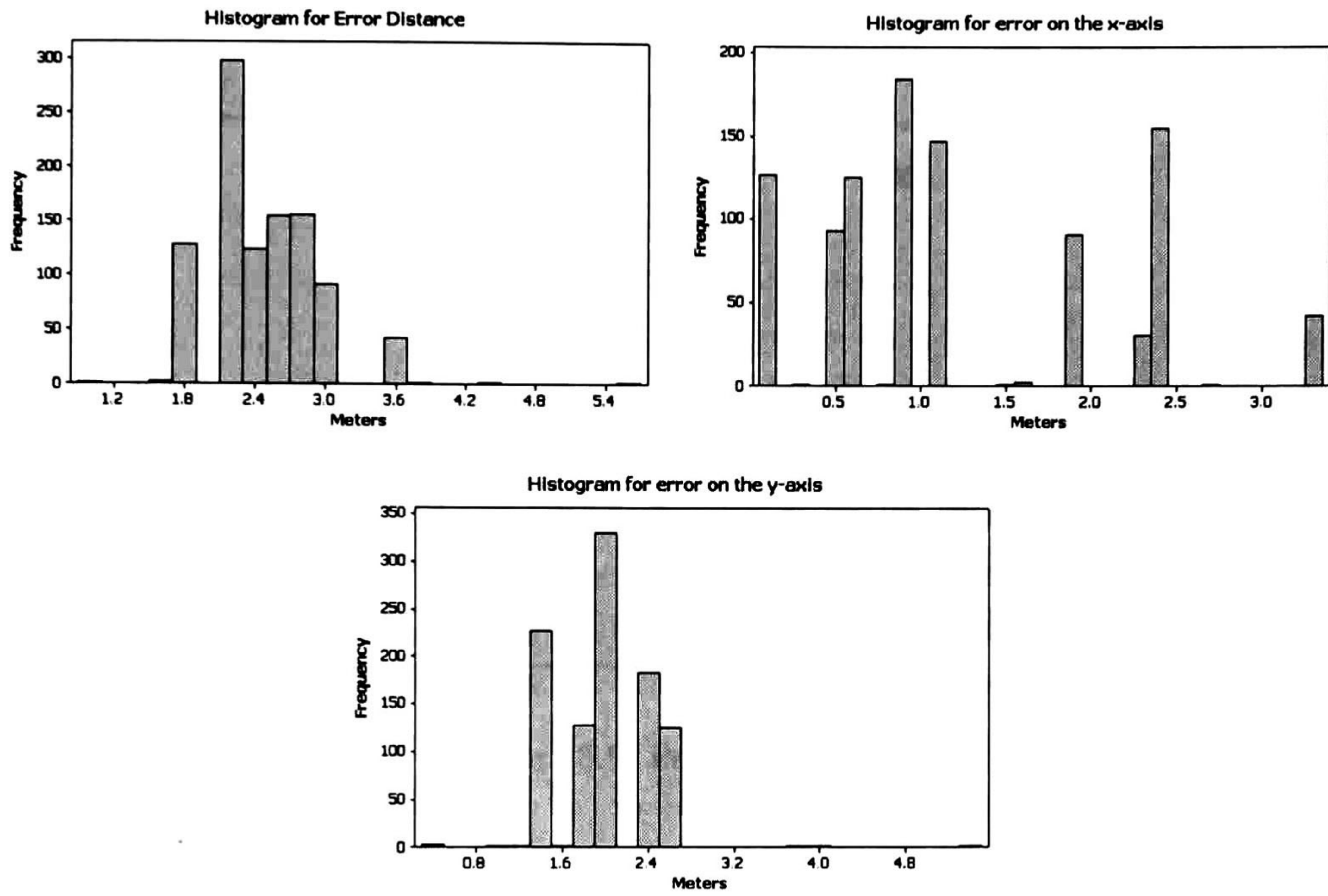


Figure 5.3: Histograms for the errors

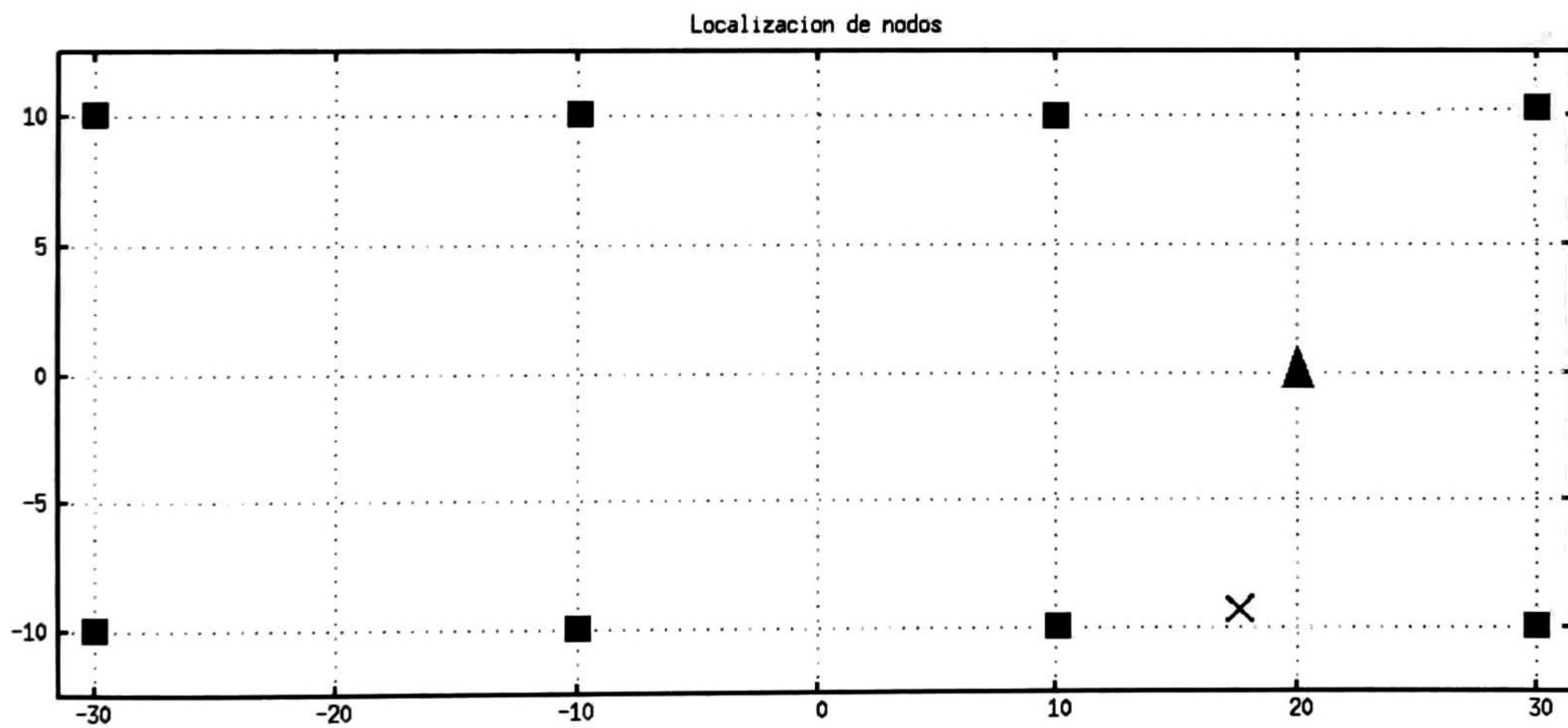


Figure 5.4: Position 1 result.

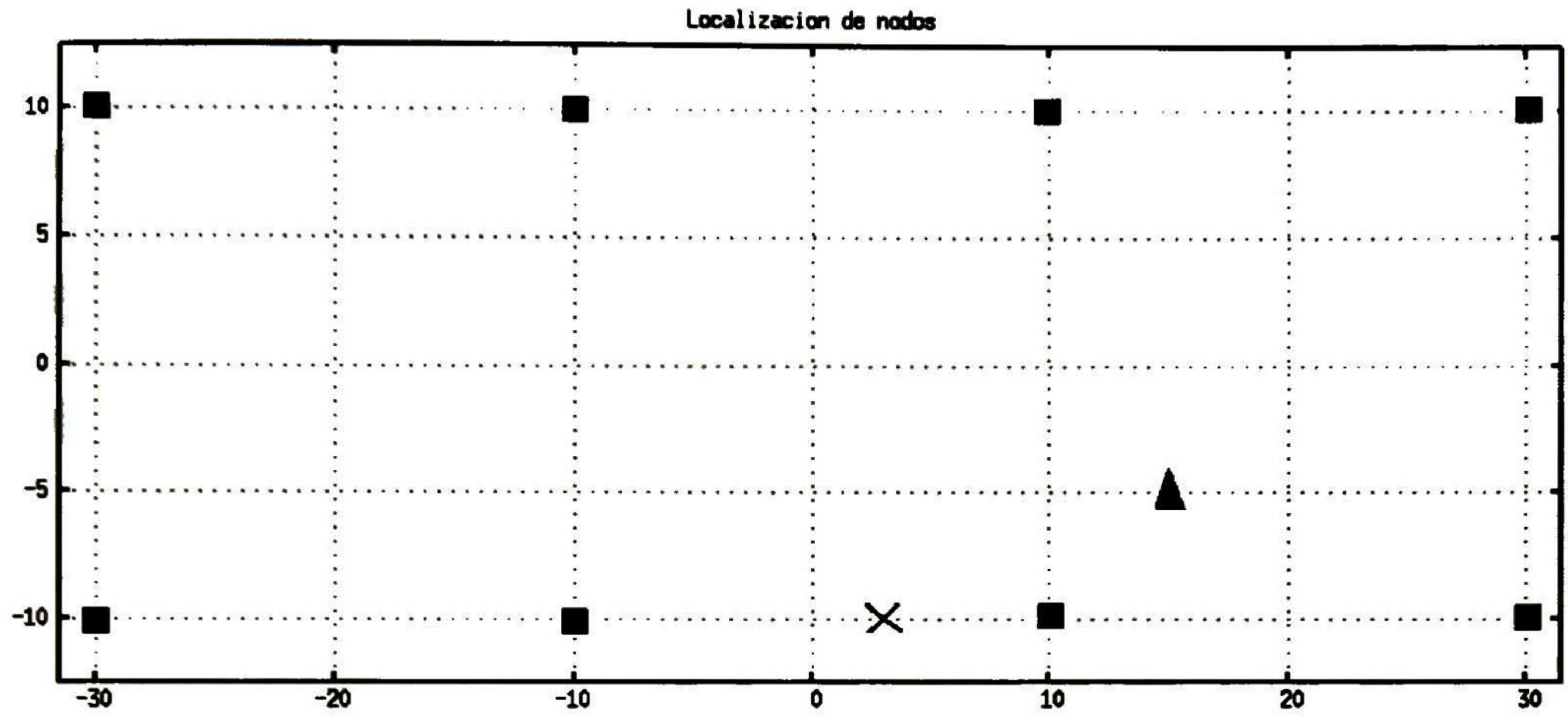


Figure 5.5: Position 2 result.

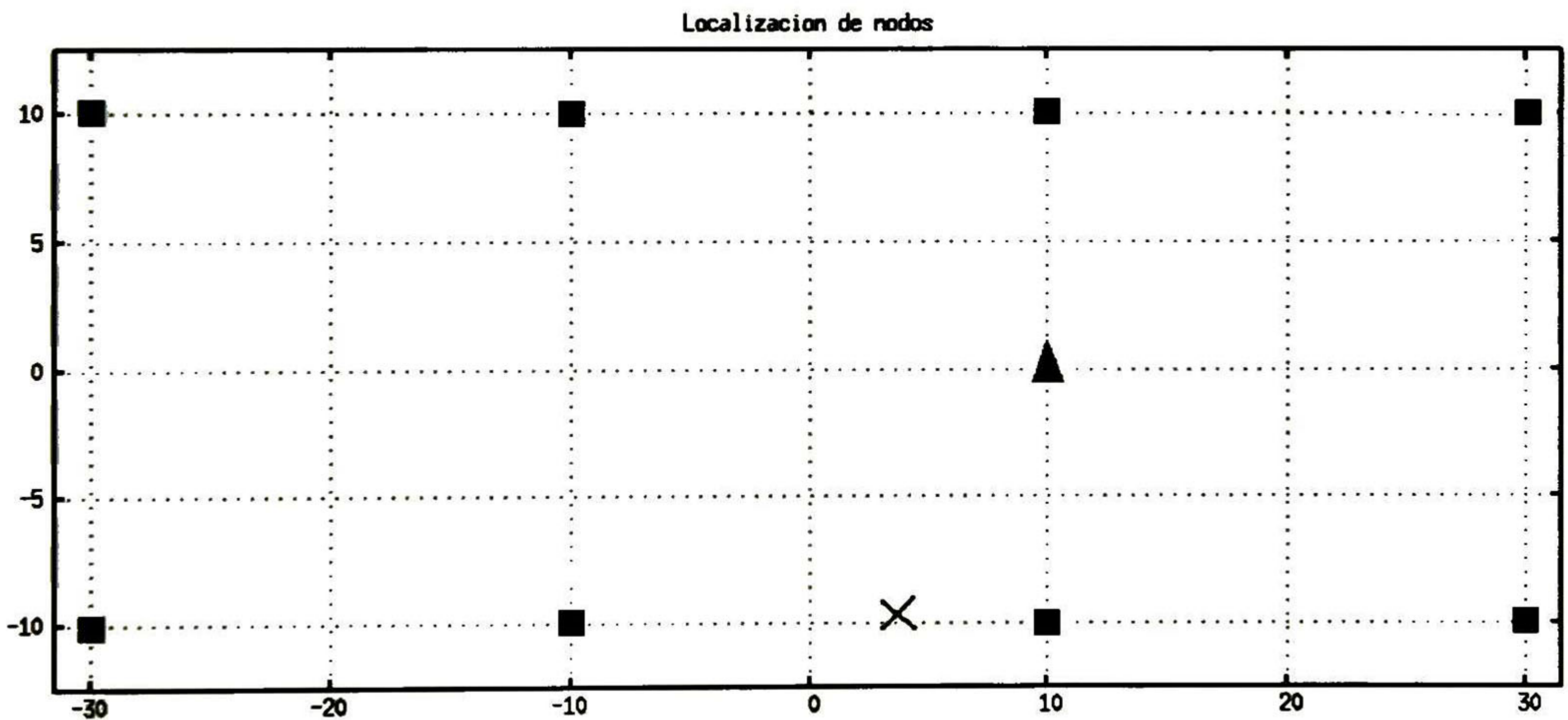


Figure 5.6: Position 3 result.

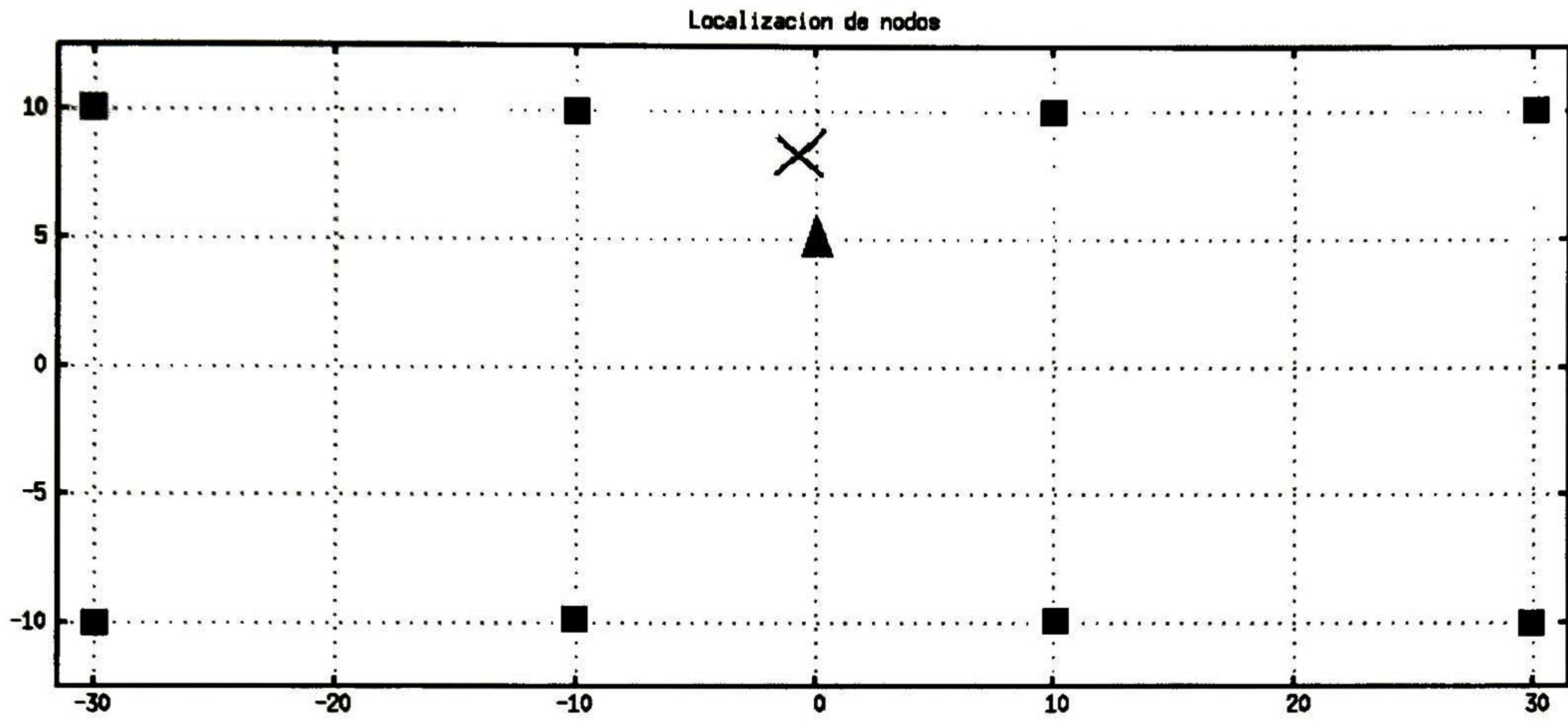


Figure 5.7: Position 4 result.

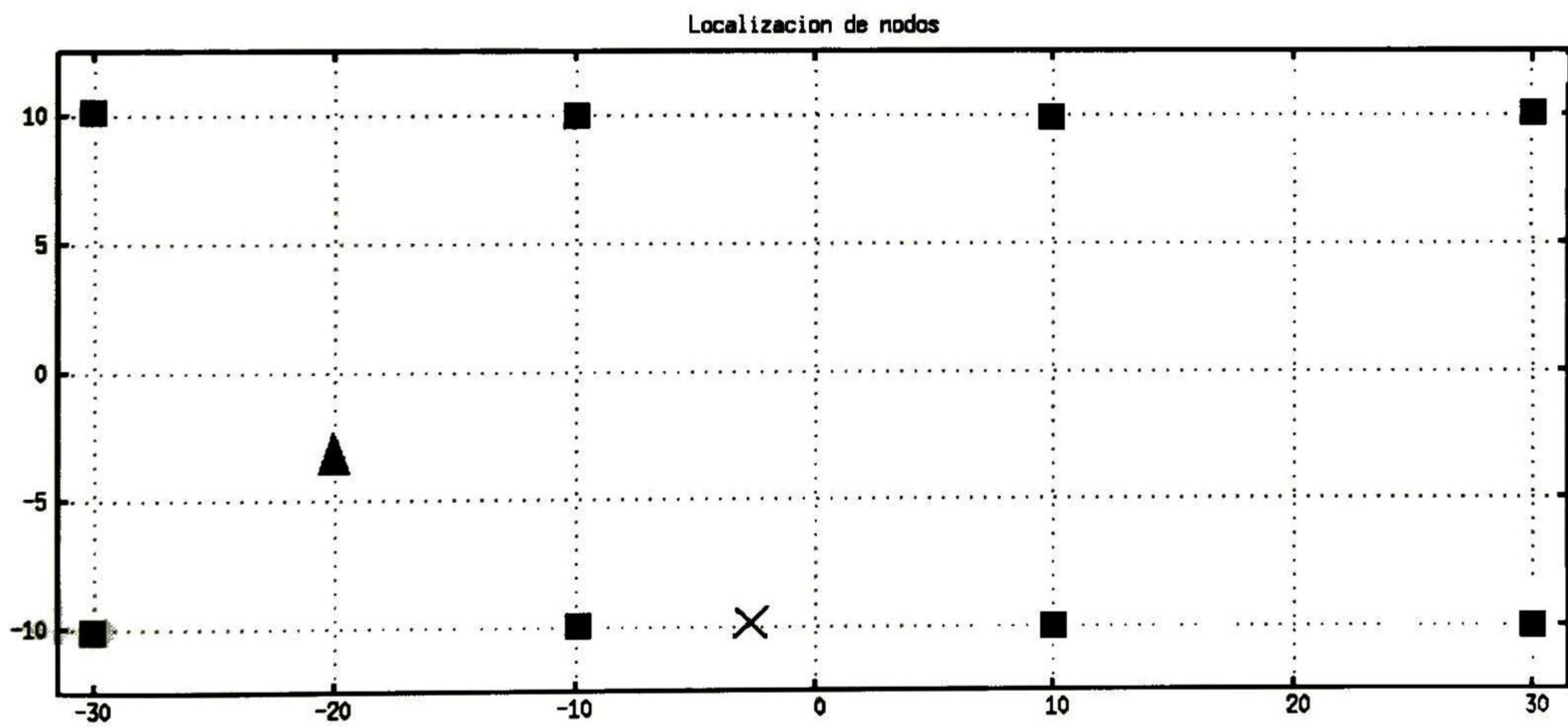


Figure 5.8: Position 5 result.

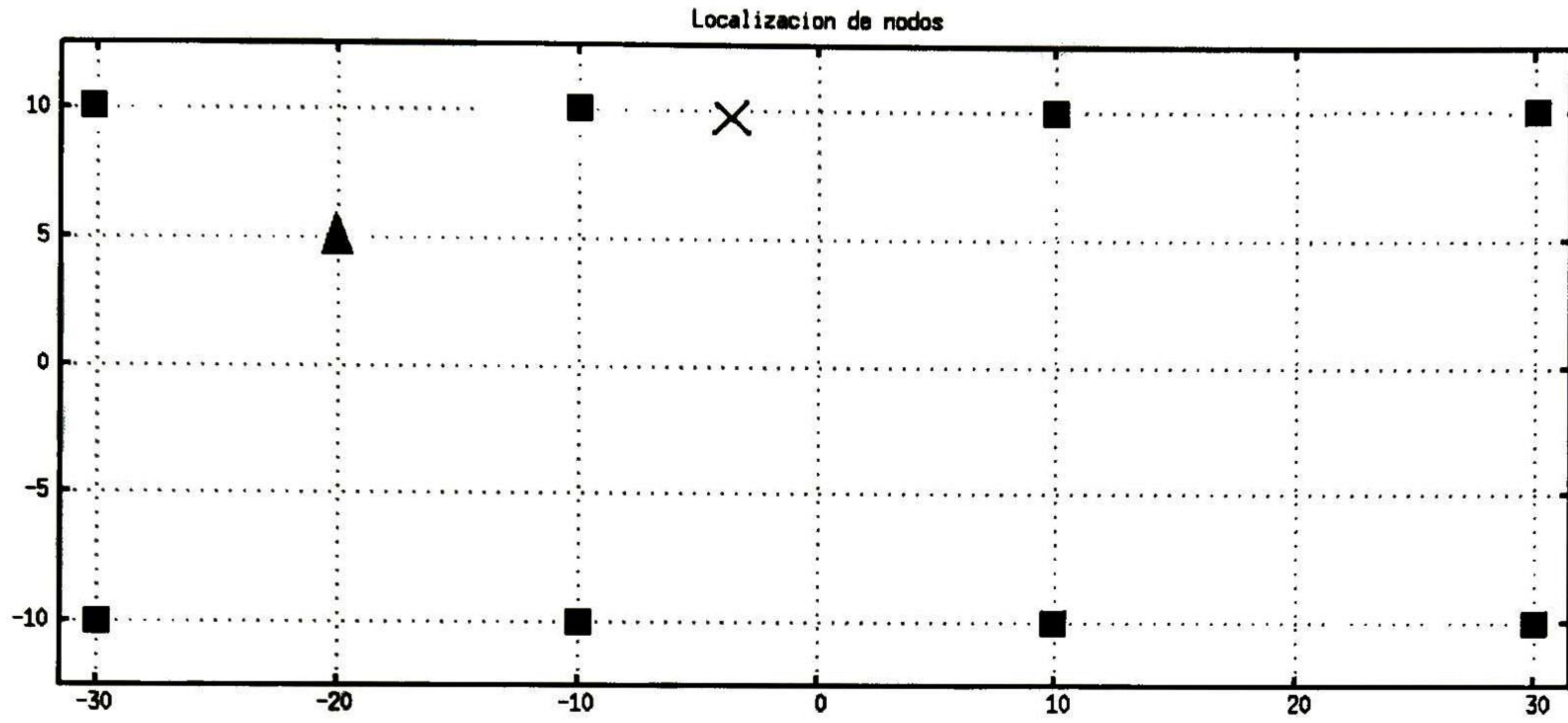


Figure 5.9: Position 6 result.

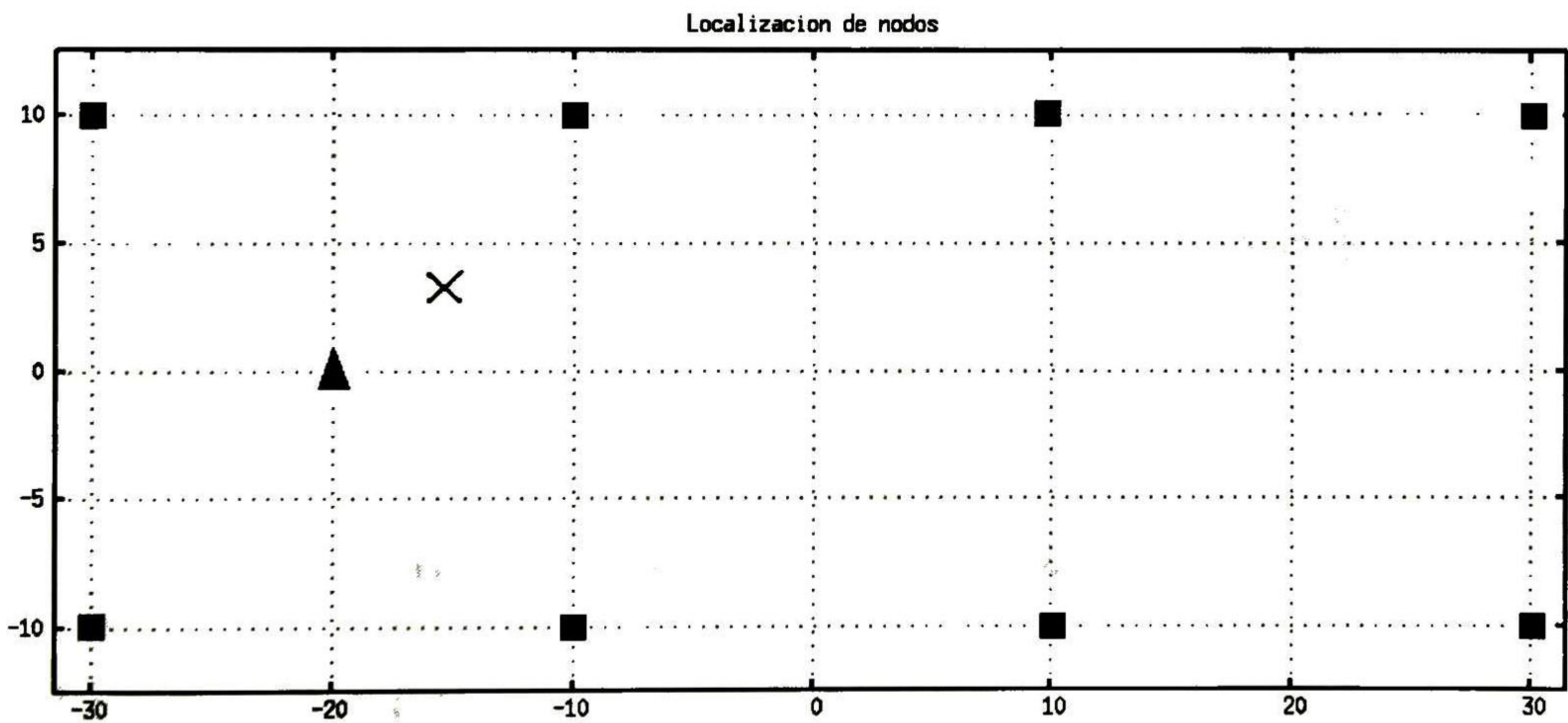


Figure 5.10: Position 7 result.

X	Y
20.0	0.0
15.0	-5.0
10.0	0.0
0.0	5.0
-20.0	-3.0
-20.0	5.0
-20.0	0.0
-15.0	-5.0

Table 5.1: Physical position of the unknown nodes

X	Y
17.71	-9.32
3.02	-9.92
3.58	-9.57
-0.70	8.29
-2.72	-9.79
-3.61	9.80
-15.46	3.30
-1.55	-9.72

Table 5.2: Estimated position for the unknown nodes

Type of error	Mean	StDev	Minimum	Maximum
Error Distance	10.59 mts	6.03 mts	3.36 mts	18.56 mts
Error on x-axis	9.13 mts	6.46 mts	0.70 mts	17.28 mts
Error on y-axis	5.839 mts	2.480 mts	3.290 mts	9.570 mts

Table 5.3: Table of errors of the field experimental work.

5.3 The algorithm without beacons

5.3.1 Simulation

For this simulation a random dBm values were generated as in the scenario with beacons. For this simulation a a serie of random dBm measurements was generated for different positions of 4 unknown nodes used and its distance between them. These positions were chosen randomly

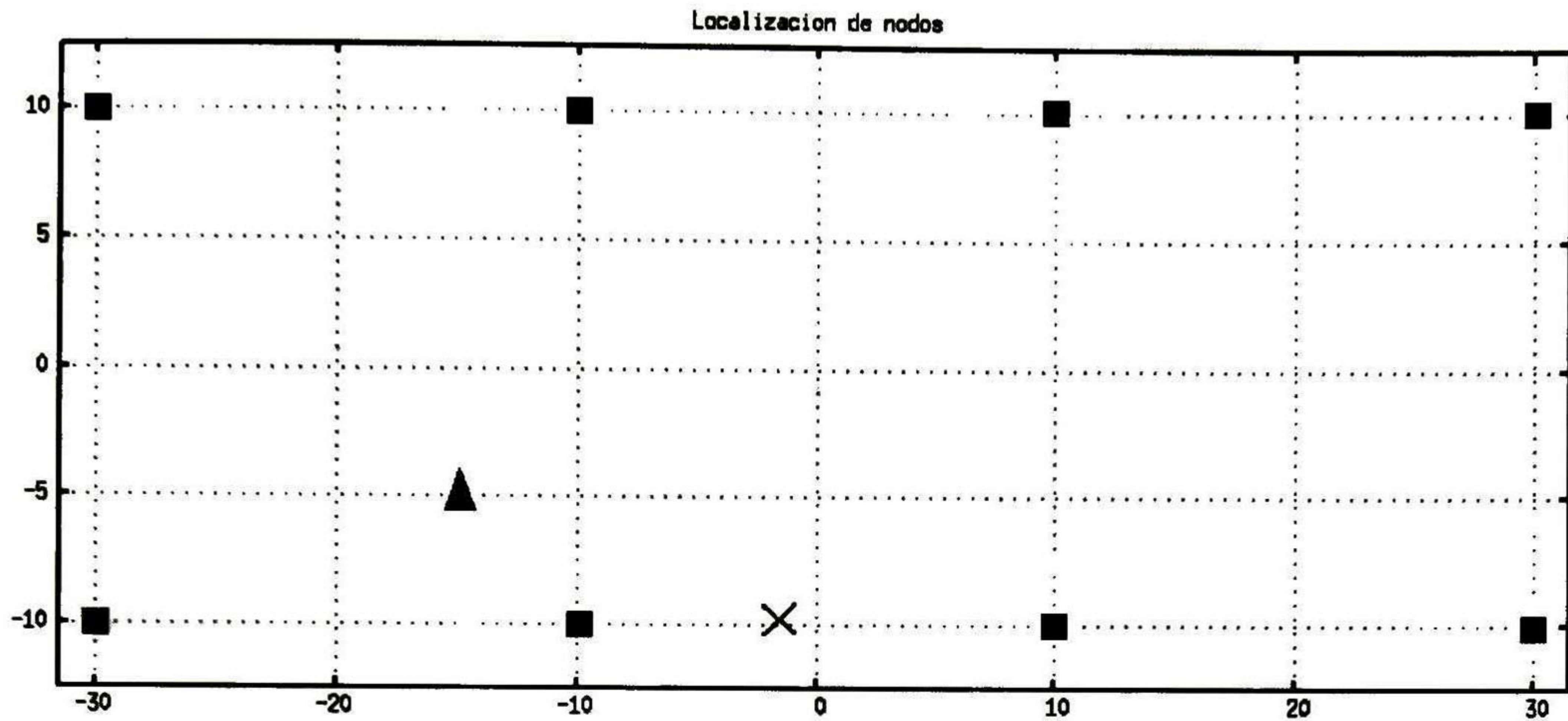


Figure 5.11: Position 8 result.

according to the layout of football pitch as shown in table 5.4, for example in figure 5.12 a run with positions $X_1=-20.0$ $Y_1=-5.0$, $X_2=0.0$ $Y_2=0.0$, $X_3=5.0$ $Y_3=5.0$, $X_4 = 10.0$ $Y_4 = -5.0$ can be seen.

X_1	Y_1	X_2	Y_2	X_3	Y_3	X_4	Y_4
-15.0	0.0	5.0	0.0	10.0	10.0	-20.0	0.0
3.0	10.0	15.0	25.0	0.0	14.0	20.0	-10.0
5.0	-15.0	10.0	-10.0	0.0	-5.0	-10.0	0.0
-20.0	-5.0	0.0	0.0	5.0	5.0	10.0	-5.0

Table 5.4: Different positions for the beaconless case

The simulation was run 1,000 times and logged in a file. An analysis was performed on the *error distance*, the *error on the x-axis* and the *error on the y-axis* for the 4 unknown nodes in this scenario. The results are summarized in tables 5.5, 5.6, 5.7.

5.4 Analysis

MDS returns node localisation in an Eucliden space between the nodes and the Radio Propagation model proposed. This configuration of points is shifted to the center of the plane with origin in 0,0 (in this case illustrated as the soccer field).

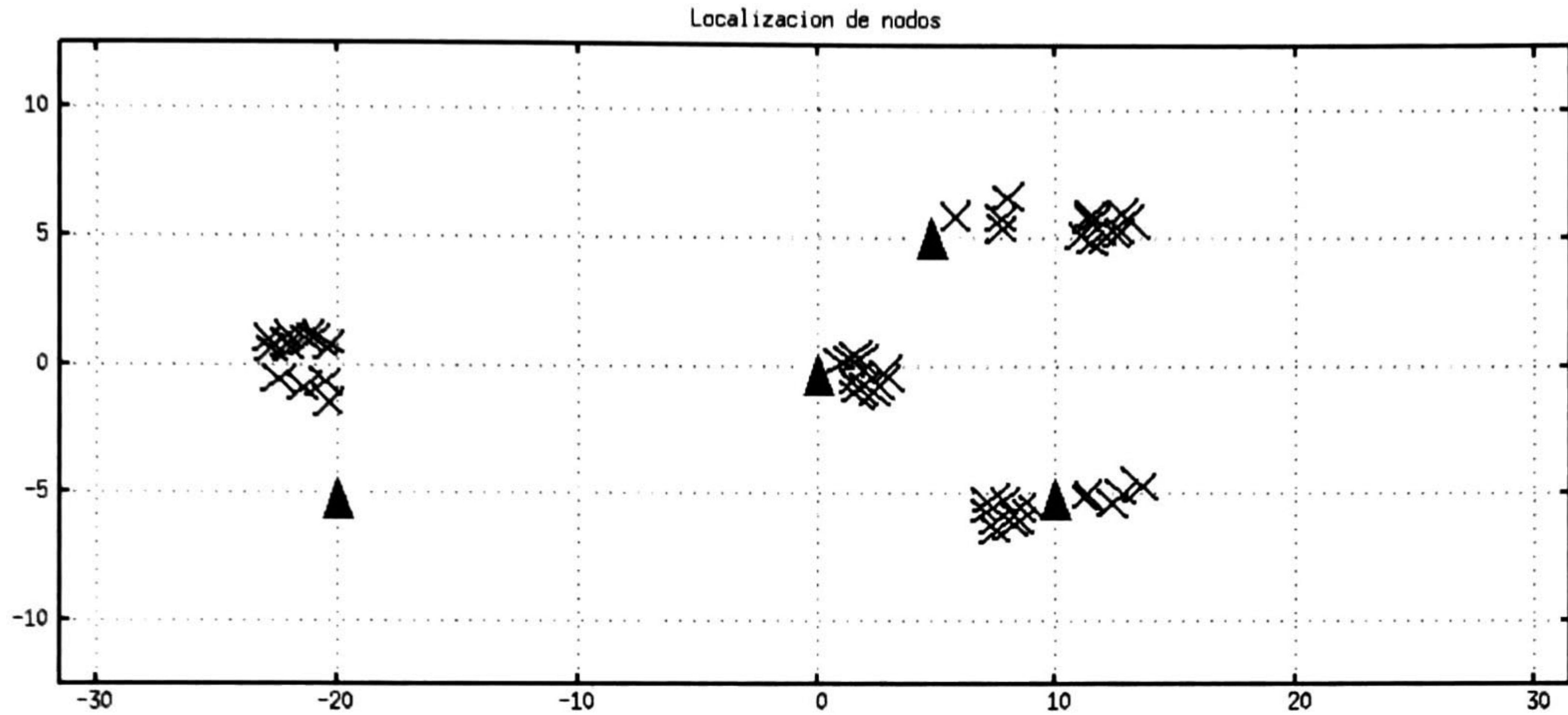


Figure 5.12: Different estimations for 4 nodes

Error Distance	Mean	StDev	Minimum	Maximum
Sensor 1	5.6606 mts	0.9283 mts	4.2484 mts	6.6637 mts
Sensor 2	1.8139 mts	0.2006 mts	0.3625 mts	2.6080 mts
Sensor 3	8.676 mts	3.923 mts	2.864 mts	11.719 mts
Sensor 4	9.194 mts	3.386 mts	1.178 mts	11.401 mts

Table 5.5: This table summarize errors of distance for the simulation

Error on x-axis	Mean	StDev	Minimum	Maximum
Sensor 1	1.7395 mts	0.8404 mts	0.2786 mts	2.9191 mts
Sensor 2	1.7057 mts	0.1572 mts	0.2156 mts	1.7119 mts
Sensor 3	2.9545 mts	0.2620 mts	2.0464 mts	3.2534 mts
Sensor 4	1.9285 mts	0.5406 mts	1.1758 mts	3.1505 mts

Table 5.6: This table summarize errors on X-axis for the simulation

It is observed from the error analysis that the further away a node is located from the plane center the bigger the error estimated is. This observation is proved with the experimental data. A low -dBm variability occurs between two point when the distance between them is greater than 44 meters (measurements decrease only 0.10 -dBm per meters). In this case it is impossible to distinguish each other.

When distance between sensors are less than 4 meters, a very high variability occurs. In

Error on y-axis	Mean	StDev	Minimum	Maximum
Sensor 1	5.3396 mts	0.8135 mts	3.9585 mts	6.1571 mts
Sensor 2	0.55411 mts	0.29934 mts	0.13564 mts	1.18850 mts
Sensor 3	7.702 mts	4.749 mts	0.411 mts	11.258 mts
Sensor 4	8.747 mts	3.935 mts	0.070 mts	11.318 mts

Table 5.7: This table summarize errors on Y-axis for the simulation

this case, it is not possible to obtain a good distance estimate.

Using the proposed model two areas of clear uncertainty can be identified in RSSI vs Distance relationship that can explain these positions error. In figure 5.13 two red boxes over the model graph are drawn.

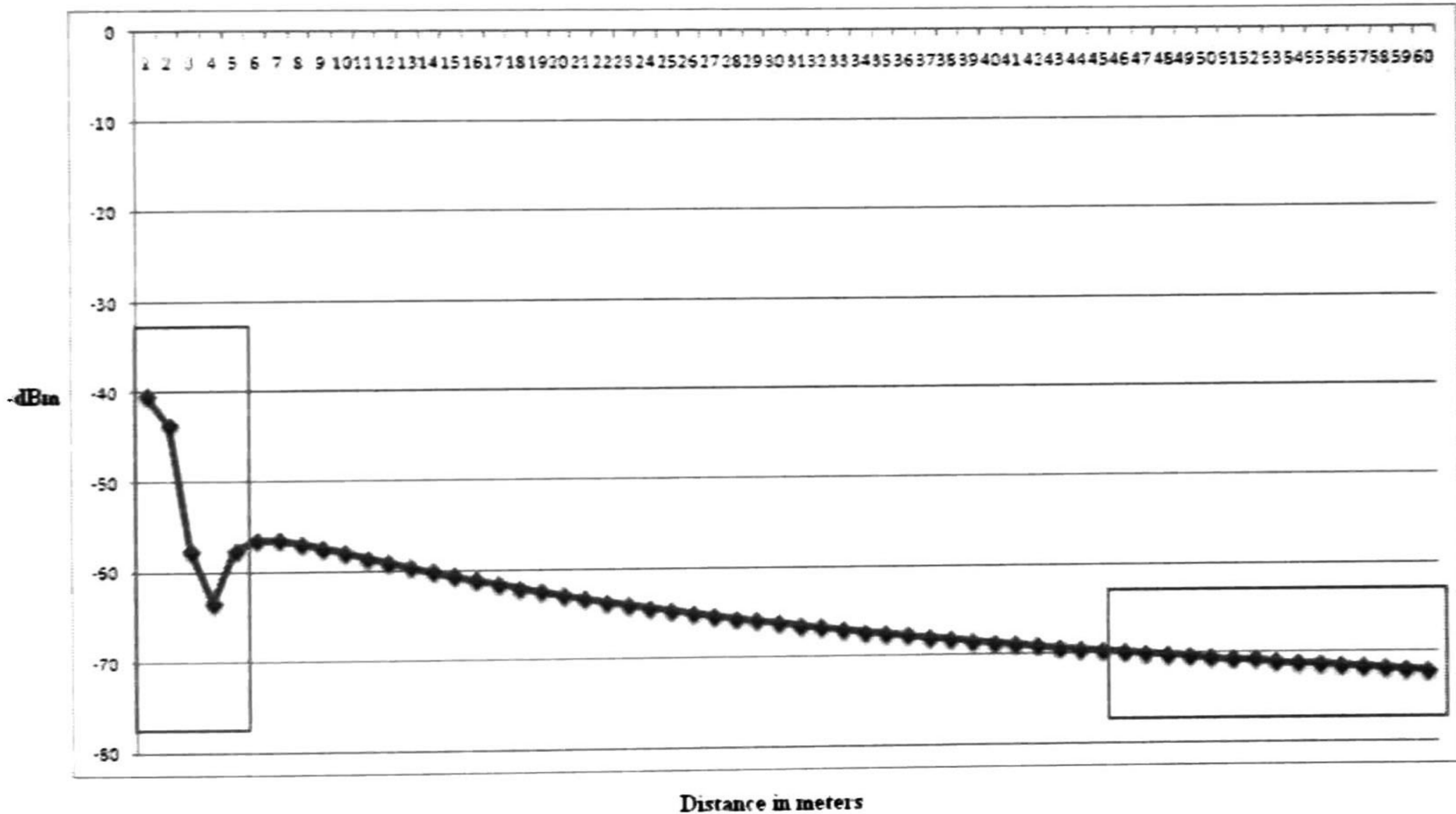


Figure 5.13: Uncertainty regions bounded by the red boxes

The first box affected by Lloyd’s Effect. This zone goes from 1 to 4 meters. This is the high variability zone. During the experiments we always tried to place to sensor at least 5 meters away from each other.

The second box bound located at the highest distance values in Figure 5.13. This zone ranges from 44 to 60 meters. This is the low variability zone and could cause that sensor position is estimated far away from the real position.

Although the objective of this work is not to produce a GPS-like system, it would be useful to make a comparison. According to [28] under ideal conditions a GPS receiver could obtain the best accuracy of 0.01 meters and a worst of only 15 meters. In [17] it is stated that that "the best practical accuracy is about 5 mts. with the current system"

5.5 Conclusions

The study of RSSI for localisation algorithms is very complex. However, zones with very high or very low variability can be identified. The proposed algorithm does not produce the desired estimation for the real cases (maximum error value 18.56 mts, minimum error value 3.36 mts). It is reasonable to think that these results can be improved by improving the accuracy of our propagation model. Based on the proposed model certainty region can also be identified.

Chapter 6

Conclusions and Future Work

6.1 Conclusions

In this thesis the major localization algorithms were reviewed. Different issues of the proposed algorithm were discussed including the hardware used for the implementation. The localisation problem was studied in two different context: with beacons and without beacons. There are solutions for both cases, but the level of accuracy will depend on the algorithm used.

An empirical study was conducted of the signal strength behavior in an outdoor environment using MC1321x zigbee radios. As a result a model for the signal propagation is proposed. This model is based on Friis Free Space Propagation model. A ground reflection phenomenon known as the Lloyd ´effect was quantified and modeled for experimental data in the 2.4 Ghz.

A summary of basic theoretical and practical facts concerning the RSSI analysis was presented. The result shown that the RSSI-based algorithms are a promise solution for node localization in known environments. The algortihm can be tailored to differents environments by changing the radio propagation model and by changing the significance level (α) for the hypotesis testing procedure.

This algorithm was implemented as a layer-2 protocol using the zigbee protocol stack due to defined primitive function already provided by by the protocol suite. Also, an brief analysis of an inverted F antenna (the antenna for MC1321x zigbee radios) was presented. This analysis revealed that the antenna orientation significantly alters the RSSI measurements.

6.2 Future Work

The wireless sensor networks area and the localization topic in particular are a new and active research area. Some open research questions still to be considered are: how cross layer network and node design can be used to improve the information quality to improve the estimation precision? How traffic characterization pattern can help us to diminish uncertainty regions for the model (this pattern includes Packet Error Rate, Bandwidth, message complexity, etc.)?

Several research directions remain active pursuing a better precision estimation. An extension to the presented research work can be made to consider 3-D scenarios. The proposed algorithm is centralized. However, an alternative approach can be considered for different applications.

The algorithm is centralized, however other approaches can be explored. However the proposed algorithm is a viable option in many deployments where a base station is already needed for different reasons.

In the signal propagation model we propose it is not possible to locate a sensor which distance is less than 4 meters (Lloyd's Effect region). A prediction tool, such as Monte Carlo, could approach this problem.

Finally, several tests under real conditions for the beaconless case are planned to perform. For this a new testbed different from the football pitch is needed.

Appendix A

MC1321x family

The MC1321x family contain an RF transceiver which is an 802.15.4 Standard-compliant radio that operates in the 2.4 GHz ISM frequency band.

RF transceiver Features:

- Fully compliant 802.15.4 Standard transceiver supports 250 kbps O-QPSK data in 5.0 MHz channels and full spread-spectrum encode and decode
- Operates on one of 16 selectable channels in the 2.4 GHz ISM band
- -1 to 0 dBm nominal output power, programmable from -27 dBm to +3 dBm typical
- Receive sensitivity of -92 dBm (typical) at 1% PER, 20-byte packet, much better than the 802.15.4 Standard of -85 dBm
- Integrated transmit/receive switch
- Dual PA output pairs which can be programmed for full differential single port or dual port operation that supports an external LNA and/or PA.
- Three low power modes for increased battery life
- Programmable frequency clock output for use by MCU
- Onboard trim capability for 16 MHz crystal reference oscillator eliminates need for external variable capacitors and allows for automated production frequency calibration
- Four internal timer comparators available to supplement MCU timer resources
- Supports both Packet Mode and Streaming Mode
- Seven GPIO to supplement MCU GPIO

The MC1321x also contains a microcontroller based on the HCS08 Family of Microcontroller Units (MCU) and can provide up to 60KB of flash memory and 4KB of RAM

Microcontroller Features:

- Low voltage MCU with 40 MHz low power HCS08 CPU core
- Up to 60K flash memory with block protection and security and 4K RAM
- MC13211: 16KB Flash, 1KB RAM
- MC13212: 32KB Flash, 2KB RAM
- MC13213: 60KB Flash, 4KB RAM
- MC13214: 60KB Flash, 4KB RAM with ZigBee Z-stack
- Low power modes (Wait plus three Stop modes)
- Dedicated serial peripheral interface (SPI) connected internally to 802.15.4 modem
- One 4-channel and one 1-channel 16-bit timer/pulse width modulator (TPM) module with selectable input capture, output capture, and PWM capability.
- 8-bit port keyboard interrupt (KBI)
- 8-channel 8-10-bit ADC
- Two independent serial communication interfaces (SCI)
- Multiple clock source options

Appendix B

Singular Value Decomposition

The singular value decomposition (SVD) is an important factorization of a rectangular real or complex matrix in linear algebra. Suppose M is an m -by- n matrix, then there exists a factorization of the form $M = U\Sigma V^*$

Where U is an m -by- m unitary matrix, the matrix Σ is m -by- n with nonnegative numbers on the diagonal (it can be seen as a n -length vector if Σ is n -by- n) and zeros off the diagonal, and V^* denotes the conjugate transpose of V , an n -by- n unitary matrix.

The singular value decomposition is very general and it can be applied to any $m \times n$ matrix. But, the eigenvalue decomposition can only be applied to certain classes of square matrices. Nevertheless, both decompositions are related. Given an SVD of M , as described above, the following two relations hold:

$$M^*M = V\Sigma^*U^*U\Sigma V^* = V(\Sigma^*\Sigma)V^*$$

$$MM^* = U\Sigma V^*V\Sigma^*U^* = U(\Sigma\Sigma^*)U^*$$

The right hand sides of these relations describe the eigenvalue decompositions of the left hand sides. Consequently, the squares of the non-zero singular values of M are equal to the non-zero eigenvalues of either M^*M or MM^* . Furthermore, the columns of U (left singular vectors) are eigenvectors of MM^* and the columns of V (right singular vectors) are eigenvectors of M^*M .

In the special case that M is a normal matrix, which by definition must be square, the spectral theorem says that it can be unitarily diagonalized using a basis of eigenvectors, so that it can be written $M = UDU^*$ for a unitary matrix U and a diagonal matrix D . When M is hermitian positive semi-definite, the decomposition $M = UDU^*$ is also a singular value decomposition.

The GNU Scientific Library subroutine `GSL_LINALG_SV_DECOMP()` offers an efficient way to compute the SVD: via the modified Golub-Reinsch algorithm (faster for matrices with

many more rows than columns), or via a one-sided Jacobi orthogonalization. Refer the GSL manual page on SVD in http://http://www.gnu.org/software/gsl/manual/html_node/Singular-Value-Decomposition.html *Singular – Value – Decomposition*.

Appendix C

Mean & StDev for 1-60 mts distance

Distance (mts.)	Mean (-dBm)	Std Dev (-dBm)
1	-40.3941	-4.112
2	-43.6274	-4.112
3	-57.5948	-4.112
4	-63.3846	-4.112
5	-57.6405	-4.112
6	-56.5907	-4.112
7	-56.5885	-4.112
8	-56.951	-4.112
9	-57.4555	-4.112
10	-58.0123	-4.112
11	-58.5814	-4.112
12	-59.1437	-4.112
13	-59.6904	-4.112
14	-60.2174	-4.112
15	-60.7233	-4.112
16	-61.2079	-4.112
17	-61.6719	-4.112
18	-62.1161	-4.112
19	-62.5417	-4.112

Table C.1: This table summarize the mean and StDev for 1 to 40 meters.

APPENDIX C. MEAN & STDEV FOR 1-60 MTS DISTANCE

Distance (mts.)	Mean (-dBm)	Std Dev (-dBm)
20	-62.9497	-4.112
21	-63.3413	-4.112
22	-63.7175	-4.112
23	-64.0794	-4.112
24	-64.4278	-4.112
25	-64.7637	-4.112
26	-65.0878	-4.112
27	-65.4009	-4.112
28	-65.7036	-4.112
29	-65.9966	-4.112
30	-66.2804	-4.112
31	-66.5555	-4.112
32	-66.8226	-4.112
33	-67.0819	-4.112
34	-67.3339	-4.112
35	-67.5791	-4.112
36	-67.8177	-4.112
37	-68.0501	-4.112
38	-68.2765	-4.112
39	-68.4974	-4.112
40	-68.7129	-4.112
41	-68.9233	-4.112
42	-69.1288	-4.112
43	-69.3296	-4.112
44	-69.526	-4.112
45	-69.7181	-4.112
46	-69.9061	-4.112
47	-70.0902	-4.112
48	-70.2706	-4.112
49	-70.4473	-4.112
50	-70.6205	-4.112
51	-70.7904	-4.112
52	-70.7904	-4.112
53	-71.1207	-4.112
54	-71.2813	-4.112
55	-71.439	-4.112
56	-71.5939	-4.112
57	-71.7461	-4.112
58	-71.8958	-4.112
59	-72.0429	-4.112
60	-72.1876	-4.112

Table C.2: This table summarize the mean and StDev for 41 to 60 meters.

Bibliography

- [1] D. Culler, D. Estrin, and M. Srivastava. Guest editors' introduction: Overview of sensor networks. *Computer*, 37(8):41–49, Aug. 2004.
- [2] Wikipedia. dbm.
- [3] Inc. Freescale Semiconductor. Compacted integrated antennas. design and application for the mc1319x, mc1320x, and mc1321x.
- [4] The Institute of Electrical and Electronics Engineers. Ieee std 802.15.4-2006, ieee standard for information technologytelecommunications and information exchange between systemslocal and metropolitan area networks.
- [5] Nissanka Bodhi Priyantha, Hari Balakrishnan, Erik Demaine, and Seth Teller. Mobile-Assisted Localization in Wireless Sensor Networks. In *IEEE INFOCOM*, Miami, FL, March 2005.
- [6] Nirupama Bulusu, John Heidemann, and Deborah Estrin. Gps-less low cost outdoor localization for very small devices. *IEEE Personal Communications Magazine*, 7(5):28–34, October 2000.
- [7] P. Bahl and V N. Padmanabhan. Radar: an in-building rf-based user location and tracking system. volume 2, pages 775–784 vol.2, 2000.
- [8] Jeffrey Hightower, Roy Want, and Gaetano Borriello. SpotON: An indoor 3d location sensing technology based on RF signal strength. UW CSE 00-02-02, University of Washington, Department of Computer Science and Engineering, Seattle, WA, February 2000.
- [9] Andrew M. Ladd, Kostas E. Bekris, Algis P. Rudys, Dan S. Wallach, and Lydia E. Kavraki. On the feasibility of using wireless Ethernet for indoor localization. *IEEE Transactions on Robotics and Automation*, 20(3):555–559, June 2004.
- [10] Theodore S. Rappaport and Theodore Rappaport. *Wireless Communications: Principles and Practice (2nd Edition)*. Prentice Hall PTR, December 2001.
- [11] J. Bachrach and C. Taylor. Localization in sensor networks. In Ivan Stojmenovic, editor, *Handbook of Sensor Networks: Algorithms and Architectures*, pages 199–237. John Wiley Sons, September 2005.

- [12] D. Niculescu and B. Nath. Ad hoc positioning system (aps). *Global Telecommunications Conference, 2001. GLOBECOM '01. IEEE*, 5:2926–2931 vol.5, 2001.
- [13] L. Doherty, K.S.J. pister, and L. El Ghaoui. Convex position estimation in wireless sensor networks. *INFOCOM 2001. Twentieth Annual Joint Conference of the IEEE Computer and Communications Societies. Proceedings. IEEE*, 3:1655–1663 vol.3, 2001.
- [14] Nirupama Bulusu, John Heidemann, and Deborah Estrin. Gps-less low cost outdoor localization for very small devices. *IEEE Personal Communications Magazine*, 7(5):28–34, October 2000.
- [15] V. Ramadurai and M. Sichitiu. Localization in wireless sensor networks: A probabilistic approach. 2003.
- [16] I. Borg and P.J.F. Groenen. *Modern Multidimensional Scaling: Theory and Applications*. 2005.
- [17] How is the accuracy of a gps receiver described.
- [18] T. Camp, J. Boleng, and V. Davies. A survey of mobility models for ad hoc network research. *Wireless Communications Mobile Computing (WCMC): Special issue on Mobile Ad Hoc Networking: Research, Trends and Applications*, 2(5):483–502, 2002.
- [19] B. Ristic, S. Arulampalam, and N. Gordon. Beyond the kalman filter: Particle filters for tracking applications. 2004.
- [20] V. Fox, J. Hightower, Lin Liao, D. Schulz, and G. Borriello. Bayesian filtering for location estimation. *Pervasive Computing, IEEE*, 2(3):24–33, July-Sept. 2003.
- [21] Frank Dellaert, Dieter Fox, Wolfram Burgard, and Sebastian Thrun. Monte carlo localization for mobile robots. In *IEEE International Conference on Robotics and Automation (ICRA99)*, May 1999.
- [22] Wolfram Burgard, Dieter Fox, Daniel Hennig, and Timo Schmidt. Estimating the absolute position of a mobile robot using position probability grids. In *AAAI/IAAI, Vol. 2*, pages 896–901, 1996.
- [23] Kai O. Arras, Jose A. Castellanos, Martin Schilt, and Roland Siegwart. Towards feature-based multi-hypothesis localization and tracking.
- [24] Reid Simmons and Sven Koenig. Probabilistic robot navigation in partially observable environments. In *Proceedings of the International Joint Conference on Artificial Intelligence*, pages 1080–1087, 1995.
- [25] John Krumm, Lyndsay Williams, and Greg Smith. Smartmovex on a graph - an inexpensive active badge tracker. In *UbiComp '02: Proceedings of the 4th international conference on Ubiquitous Computing*, pages 299–307, London, UK, 2002. Springer-Verlag.
- [26] Inc. Freescale Semiconductor. Simple media access controller (smac) users guide.
- [27] David C. Lay. *Linear algebra and its applications*. 1993.

- [28] Accuracy of gps.



CENTRO DE INVESTIGACIÓN Y DE ESTUDIOS AVANZADOS DEL I.P.N. UNIDAD GUADALAJARA

El Jurado designado por la Unidad Guadalajara del Centro de Investigación y de Estudios Avanzados del Instituto Politécnico Nacional aprobó la tesis

Algoritmo de Localización de Nodos en Redes de Sensores
Inalámbricas Basado en un Modelo Probabilístico y de Escalamiento
Multidimensional

del (la) C.

Ernesto NAVARRO ALVAREZ

el día 26 de Septiembre de 2008.

Dr. Pablo Moreno Villalobos
Investigador CINVESTAV 3C
CINVESTAV Unidad Guadalajara

Dr. Juan Manuel Ramírez Arredondo
Investigador CINVESTAV 3C
CINVESTAV Unidad Guadalajara

Dr. Félix Francisco Ramos Corchado
Investigador CINVESTAV 3A
CINVESTAV Unidad Guadalajara

Dr. Mario Angel Siller González
Pico
Investigador CINVESTAV 2A
CINVESTAV Unidad Guadalajara



CINEVESTAV
BIBLIOTECA CENTRAL



SSIT000006888